

PROPAGATION OF MICROWAVES ON A SINGLE WIRE—PART I

BY S. K. CHATTERJEE AND P. MADHAVAN

(*Department of Electrical Communication Engineering, Indian Institute of Science,
Bangalore-3*)

Received April 26, 1955

ABSTRACT

Some quantitative measurements on cylindrical surface waves excited on a cylindrical bare copper conductor have been made at 3.2 cm. wavelength. The results on radial field measurements indicate fair agreement with results predicted by theory. The decay coefficient for the radial field is 14.0 m^{-1} . It is suggested that the surface conductivity of metals in the form of wire can be found at microwave frequencies by using this method. Field distributions near the launching horn have been found to be considerably distorted due probably to the presence of complementary waves. The design and constructional details of the launching system, probe, etc. used in the experiment are presented.

SURFACE WAVE

The paper forms a part of a series of investigations on surface wave transmission at microwave frequencies. In view of the growing importance of the subject and considerable discussions on the physical reality of surface waves in recent years, it is considered worthwhile to present at the outset a brief but unified discussion on surface wave phenomena.

In his theory on radio wave propagation from an Hertzian dipole, Sommerfeld introduced two new terms 'surface wave' and 'space wave', in addition to the two already familiar terms 'induction' and 'radiation' fields. Surface wave may be conveniently classified as (i) an inhomogeneous plane wave supported by a flat surface. This is the same as 'Zenneck wave', (ii) a radial cylindrical surface wave supported by a flat surface, and (iii) an axial cylindrical surface wave supported by a homogeneous cylindrical surface immersed in a homogeneous dielectric. This is the same as Sommerfeld-Goubau wave.

Zenneck (1907) showed that Maxwell's field equations admit a solution which may be interpreted as a surface wave guided by a plane interface separating two homogeneous media of different permittivity and conductivity. It was not indicated by Zenneck whether such a wave could be generated by an antenna. If the interface lying in the xy -plane at $z = 0$ separates two homogeneous media

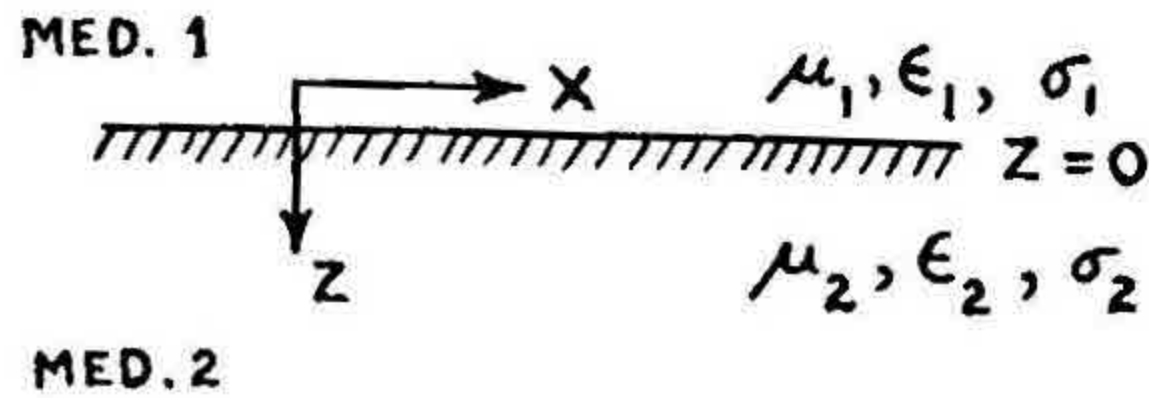


FIG. 1. Interface lying in the xy -plane at $z=0$.

and the direction of propagation is as shown in Fig. 1, the Zenneck wave is represented by the field components as follows:—

For $z \geq 0$, i.e., outside the surface

$$\begin{aligned} E_{z1} &= -A \frac{\gamma_1}{\sigma_1 + j\omega\epsilon_1} F_1 e^{-\gamma x} \\ E_{x1} &= A \frac{\gamma}{\sigma_1 + j\omega\epsilon_1} F_1 e^{-\gamma x} \\ H_{y1} &= A F_1 e^{-\gamma x} \end{aligned} \tag{1}$$

For $z \leq 0$, i.e., inside the surface

$$\begin{aligned} E_{z2} &= A \frac{\gamma_2}{\sigma_2 + j\omega\epsilon_2} F_2 e^{-\gamma x} \\ E_{x2} &= A \frac{\gamma}{\sigma_2 + j\omega\epsilon_2} F_2 e^{-\gamma x} \\ H_{y2} &= A F_2 e^{-\gamma x} \end{aligned} \tag{2}$$

where,

$$\begin{aligned} F_1 &= \exp(j\omega t - \gamma_1 z) \\ F_2 &= \exp(j\omega t + \gamma_2 z) \end{aligned}$$

and A is the excitation constant.

The radial form of surface wave supported by a flat surface has the following non-vanishing components.

For $z \geq 0$

$$\begin{aligned} E_{r1} &= A \frac{\gamma_1}{\sigma_1 + j\omega\epsilon_1} F_1 H_1^{(2)}(-j\gamma r) \\ E_{\theta 1} &= A \frac{\gamma}{\sigma_1 + j\omega\epsilon_1} F_1 H_0^{(2)}(-j\gamma r) \\ H_{\theta 1} &= A F_1 H_1^{(2)}(-j\gamma r) \end{aligned} \tag{3}$$

For $z \leq 0$

$$\begin{aligned} E_{r_2} &= -A \frac{\gamma_2}{\sigma_2 + j\omega\epsilon_2} F_2 H_1^{(2)}(-j\gamma r) \\ E_{z_2} &= A \frac{j\gamma}{\sigma_2 + j\omega\epsilon_2} F_2 H_0^{(2)}(-j\gamma r) \\ H_{\theta_2} &= A F_2 H_1^{(2)}(-j\gamma r) \end{aligned} \quad (4)$$

When $r \rightarrow \infty$, H 's $\rightarrow e^{-\gamma r}/\sqrt{r}$ and the radial surface wave becomes identical with the Zenneck wave.

Sommerfeld (1909, 1926) formulated the wavefunctions for a vertical infinitesimal dipole as an infinite integral and explained that the surface wave component is contained in the integral taken around the pole of the integrand. This led to the conclusion that a transversely cylindrical surface immersed in air would support a surface wave. Weyl (1919) obtained a solution which could be considered as the superposition of a surface and a space wave, but the solution did not contain explicitly any surface wave component. The evaluation of Sommerfeld's formulæ by Rolf (1930) yielded results which differed from the formulæ of Weyl and Norton (1935) by exactly the surface wave component. This led to the question about the physical reality of surface wave (Burrows, 1936). Kahan and Eckart (1949) pointed out that Sommerfeld's evaluation of the integral along the branch cut is in error. A correct evaluation of the integral yields an expression which contains two surface wave components of opposite sign and hence it is concluded that Sommerfeld's surface wave does not exist in the radiation of a Hertzian dipole over a plane earth. This agrees with the discussion of Bowkamp (1950) and the solution of Weyl. This is also in conformity with the solution of Wise (1937) and Rice (1937) and has been confirmed by the experimental results of Burrows (1937).

SOMMERFELD-GOUBAU WAVE

The present paper is concerned with a non-radiating mode (Sommerfeld, 1899; Goubau, 1950) propagating along the length of a solid cylindrical wire immersed in air. The propagation characteristics of a wave guided by a cylindrical conductor of radius a immersed in an infinite homogeneous medium is determined by solving the following equation (Stratton, 1941).

$$\begin{aligned} &\left[\frac{\mu_2}{\lambda_2 a} \frac{J_n'(\lambda_2 a)}{J_n(\lambda_2 a)} - \frac{\mu_1}{\lambda_1 a} \frac{H_n^{(1)'}(\lambda_1 a)}{H_n^{(1)}(\lambda_1 a)} \right] \\ &\times \left[\frac{\gamma_2^2}{\mu_2 \lambda_2 a} \frac{J_n'(\lambda_2 a)}{J_n(\lambda_2 a)} - \frac{\gamma_1^2}{\mu_1 \lambda_1 a} \frac{H_n^{(1)'}(\lambda_1 a)}{H_n^{(1)}(\lambda_1 a)} \right] = \frac{n^2 h^2}{a^2} \left(\frac{1}{\lambda_1^2} - \frac{1}{\lambda_2^2} \right)^2 \end{aligned} \quad (5)$$

where,

$$\lambda_1^2 = \gamma_1^2 - h^2$$

$$\lambda_2^2 = \gamma_2^2 - h^2$$

The roots of this equation which determine the propagation factor h_{nm} are discrete. An infinite number of symmetric and asymmetric E and H waves arises from the solution for propagation constant. If the conductivity of the conductor is infinite, the boundary condition can be fulfilled by either a E or a H wave. If however, the conductivity is finite, the boundary condition can be fulfilled by only an hybrid EH wave except in the case when the wire is excited by a circular symmetric mode. In the case of copper wire, the conductivity is sufficiently high so as to enable the excitation of either E or H wave. Asymmetric modes are also excited (Hondros, 1909) along with the symmetric modes but they are rapidly attenuated within a short distance from the source and consequently play insignificant part in the propagation of wave along a cylindrical conductor. For an axially symmetric H wave, there is no principal wave having low attenuation. Consequently, the axially symmetric H wave is rapidly damped out (Sommerfeld, 1904). The only mode of importance then is the axially symmetric E wave which is characterised by relatively low attenuation and has its characteristic equation derived from (5) as follows:—

$$\frac{H_0^{(1)}(\gamma_1 a)}{H_1^{(1)}(\gamma_1 a)} = 0 \quad (6)$$

In order that a surface wave may be propagated along a cylindrical conductor, the propagation constant γ_1 must be related to the eigenfactor k_o as follows:—

$$\gamma_1 = \pm j\omega \sqrt{\mu_1 \epsilon_1 + \frac{k_o^2}{\omega^2}} \quad (7)$$

where

$$k_o^2 = \frac{1}{H_\theta} \frac{\partial J_x}{\partial r}$$

where J_x is the x-component of the displacement current density. The equation shows that in order that surface wave transmission is possible, the phase velocity of the guided wave must be less than the free-space velocity of electromagnetic wave in an unbounded medium. In the case of the single conductor transmission, the resistance of the wire produces a reduction in phase velocity. The surface resistance of the wire is therefore principally responsible for supporting surface wave on single wire. The surface wave field distribution is determined from the following non-vanishing field components.

For $z \geq 0$

$$\begin{aligned} E_{z1} &= A H_0^{(1)}(j\gamma_1 r) e^{j\omega t - \gamma x} \\ E_{r1} &= A \frac{\gamma}{j\gamma_1} H_1^{(1)}(j\gamma_1 r) e^{j\omega t - \gamma x} \\ H_{\theta 1} &= A \frac{\omega \epsilon_1}{\gamma_1} H_1^{(1)}(j\gamma_1 r) e^{j\omega t - \gamma x} \end{aligned} \quad (8)$$

For $z \leq 0$

$$\begin{aligned} E_{z2} &= AJ_0(j\gamma_2 r) e^{j\omega t - \gamma x} \\ E_{r2} &= A \frac{\gamma}{j\gamma_2} J_1(j\gamma_2 r) e^{j\omega t - \gamma x} \\ H_{\theta 2} &= A \frac{\sigma_2 + j\omega \epsilon_2}{j\gamma_2} J_1(j\gamma_2 r) e^{j\omega t - \gamma x} \end{aligned} \quad (9)$$

where,

$$\begin{aligned} \gamma^2 + \gamma_1^2 &= -\omega^2 \mu_1 \epsilon_1 \\ a_1 &= \text{radial decay coefficient} \\ a &= \text{axial attenuation coefficient} \\ \beta_1 &= \text{radial phase coefficient} \\ \beta &= \text{axial phase coefficient} \\ \gamma_1 &= \text{radial propagation coefficient} = a_1 - j\beta_1 \\ \gamma &= \text{axial propagation coefficient} = a + j\beta. \end{aligned}$$

The above field components show that in the plane normal to the axis of the conductor, the electromagnetic field extends to infinity in the radial direction. But it can be shown with the help of the Poynting vector that the energy density of the field decays monotonically in the radial direction, at a rate determined by the properties and conditions of the surface of the guide. At large distances from the conductor, the decay is exponential and usually most of the energy of the wave is constrained to flow in the vicinity of the wire. For large arguments, the Sommerfeld-Goubau wave becomes identical in form to the Zenneck wave. It is concluded (Burlow and Cullen, 1953) that all surface waves are basically one and the same phenomenon.

FIELD DISTRIBUTION

The non-vanishing components for the Sommerfeld-Goubau waves are E_{z1} , E_{r1} , $H_{\theta 1}$ (equation 8). The field distribution is shown in Fig. 2. The field plot

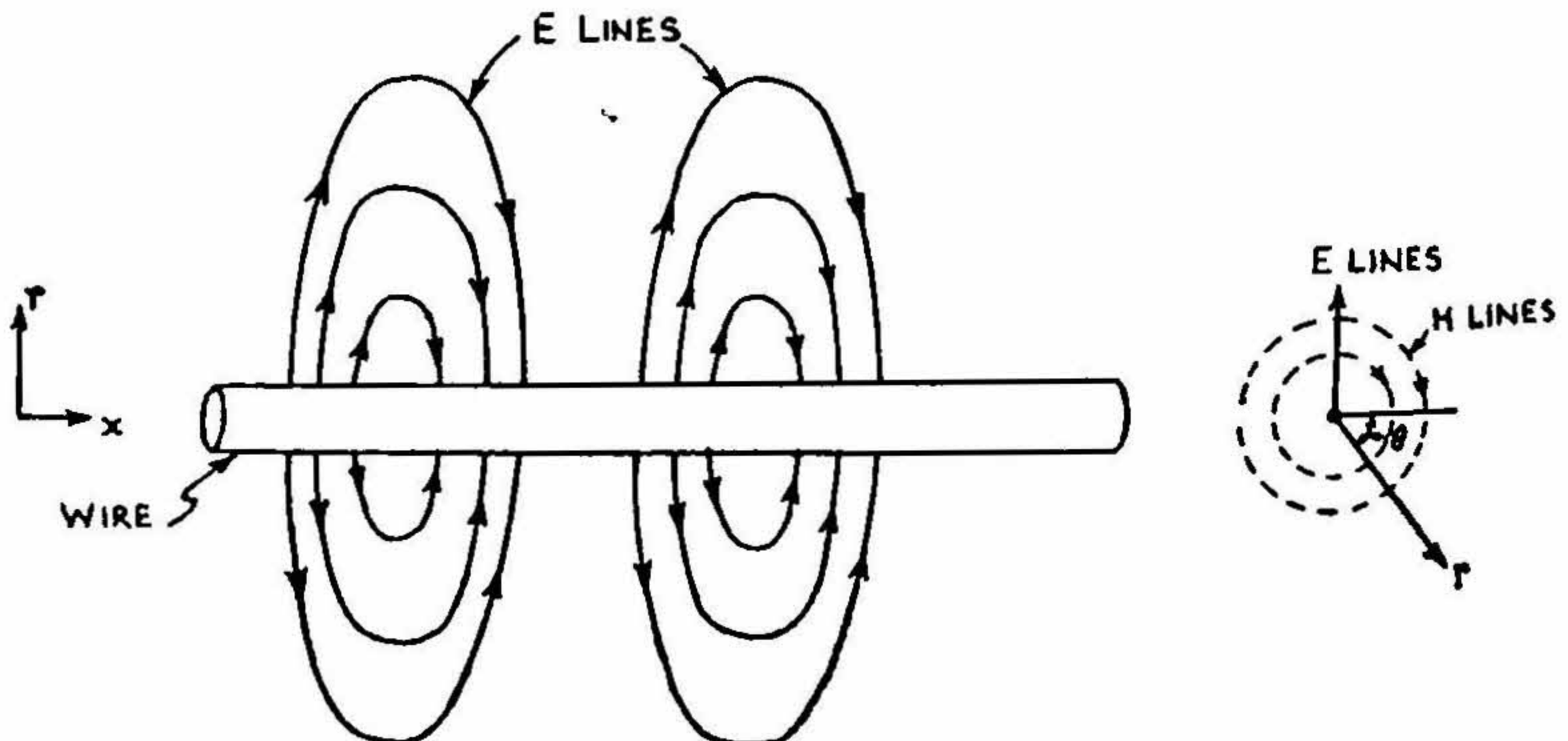


FIG. 2. Field Distribution of Sommerfeld-Goubau Wave.

shows a similarity with the field distribution in a coaxial cylindrical guide excited in a circular symmetric transverse magnetic mode.

RADIAL FIELD SPREAD

The radial propagation coefficient $\gamma_1 = \alpha_1 - j\beta_1$ in equation (8) determines the rate of decrease of field in the radial direction and also the reduction in phase velocity. In other words, γ_1 determines the radial extension of the field. The greater the value of γ_1 , the greater is α_1 and hence the radial spread of the field becomes less with increasing γ_1 . Also, with increasing value of γ_1 , the phase velocity becomes smaller. For a good conductor like copper, the ratio E_r/H_θ is small and hence γ_1 is small; consequently, a large radial field spread is expected in the case of bare copper wire used as a surface wave transmission line.

For $\gamma_1 r \rightarrow 0$, $H_1^{(1)} \propto 1/r$ and for large values of $\gamma_1 r$, $H_1^{(1)} \propto \frac{e^{-\gamma r}}{\sqrt{r}}$. Therefore, in the neighbourhood of the wire field decay follows an inverse distance law and for large distances from the wire the field decay follows an exponential law. The large extension of the field in the radial direction creates practical difficulties in setting up such a system for long distance transmission, as any obstacle present within the region of field will act as a source of scattering and hence will distort the field. It is necessary therefore, to have a knowledge of field distribution of the field in the radial direction.

The total energy flow P outside the wire of radius a is

$$P = \operatorname{Re} \int_0^\infty \int_0^{2\pi} r E_r H_\theta^* d\theta dr.$$

The energy flow at any radial distance $r = r'$ is

$$P_{r'} = \operatorname{Re} \int_{r'}^\infty \int_0^{2\pi} r E_r H_\theta^* d\theta dr.$$

The fraction of the total power constrained to flow within a radial distance r' of the wire is determined (Goubau, *loc. cit.*) approximately from the following equation:

$$\frac{P_{r'}}{P} \cong 1 + \frac{2 \log (r'/a)}{\log 2 \cdot 2 |\xi|} \quad (10)$$

where,

$$|\xi| \ln |\xi| = -|\eta| \quad (11)$$

For a copper conductor immersed in air

$$|\eta| = 1.70 \times 10^{-3} a/\lambda^{3/2} \quad (12)$$

where λ and a are in cm. The values of ξ for different values of η , *i.e.*, for different values of radii of the transmission line and λ can be theoretically computed from the graph $|\xi|$ vs. $|\eta|$ given by Goubau (*loc. cit.*). The theoretical curve between

the relative percentages of power contained within circles of different radial distances has been calculated for 12 s.w.g. bare copper conductor used in the experiment, from equation (10) and is given in Fig. 3.

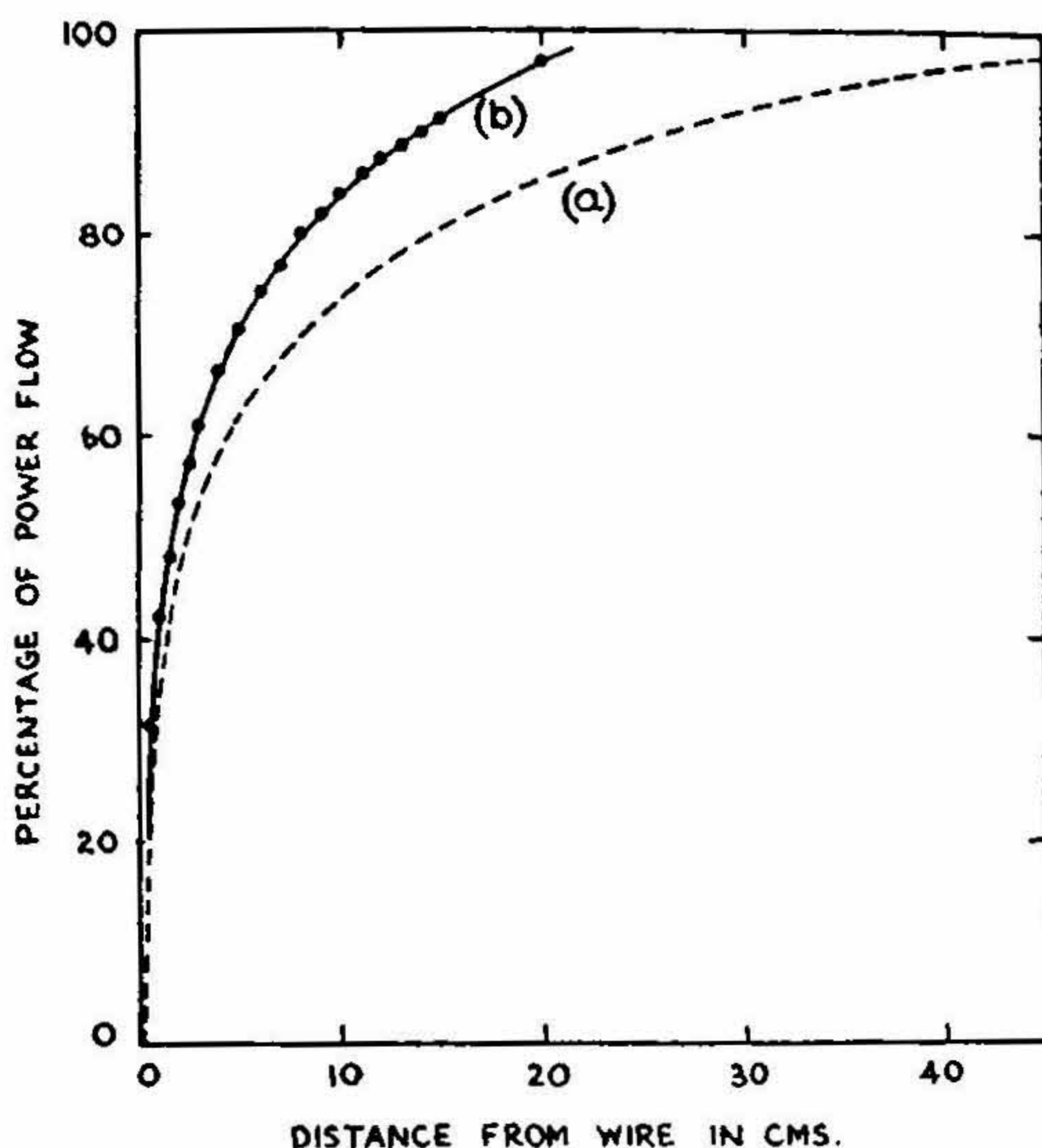


FIG. 3. Energy Distribution Curve.

(a) Curve calculated from Goubau's Relation Eq. (10) to (12): $\xi = 2.85 \times 10^{-6}$.

(b) Experimental Curve: $\xi = 1.25 \times 10^{-5}$.

It has been suggested by Harms (1907) and shown by Goubau (*loc. cit.*), that the phase velocity and hence the radial field spread can be reduced by coating the wire with dielectric or modifying the surface of the wire. It has also been shown by Kaden (1951) that the phase velocity can be reduced by using a stranded wire as a transmission line. It is one of the primary objects of the present series of investigations to find a suitable means which would shrink the radial field to almost the diameter of the wire without introducing appreciable loss.

EXPERIMENTAL

(i) *Launching of surface wave.*—A cylindrical surface wave can be efficiently excited (Goubau, 1951; Dyot, 1952) on a cylindrical conductor by means of a coaxial cable, the outer conductor of which is flared in the form of a conical horn and the inner conductor is extended to the far end as a transmission line. The non-vanishing field components describing the field inside a conical horn without the central conductor for axially symmetric transverse magnetic mode are (Buchholz, 1940; Schorr, Beck, 1950).

$$\begin{aligned}
 E_r &= A \frac{n(n+1)}{r^{3/2}} H^{(2)}_{n+1/2}(\gamma_1 r) P_n(\cos \theta) \\
 E_\theta &= \left[\frac{1}{2r^{3/2}} H^{(2)}_{n+1/2}(\gamma_1 r) + \frac{\gamma_1}{r^{1/2}} H^{(2)}_{n+1/2}(\gamma_1 r) \right] A P'_n(\cos \theta) \\
 H_\phi &= \frac{-j\omega\epsilon}{cr^{1/2}} H^{(2)}_{n+1/2}(\gamma_1 r) A P'_n(\cos \theta)
 \end{aligned}
 \tag{13}$$

The H's and P's represent Hankel function of the second kind and associated Legendre function of the first kind respectively. The Hankel function of the first kind has been omitted as it represents a wave travelling inwards. The Legendre function of the second kind has been omitted as it has a singularity on the polar axis which is contained in the region considered. The primes indicate the first derivative with respect to the argument. A and C are excitation constants.

The non-vanishing field components for the cylindrical conductor excited by E_{01} wave are

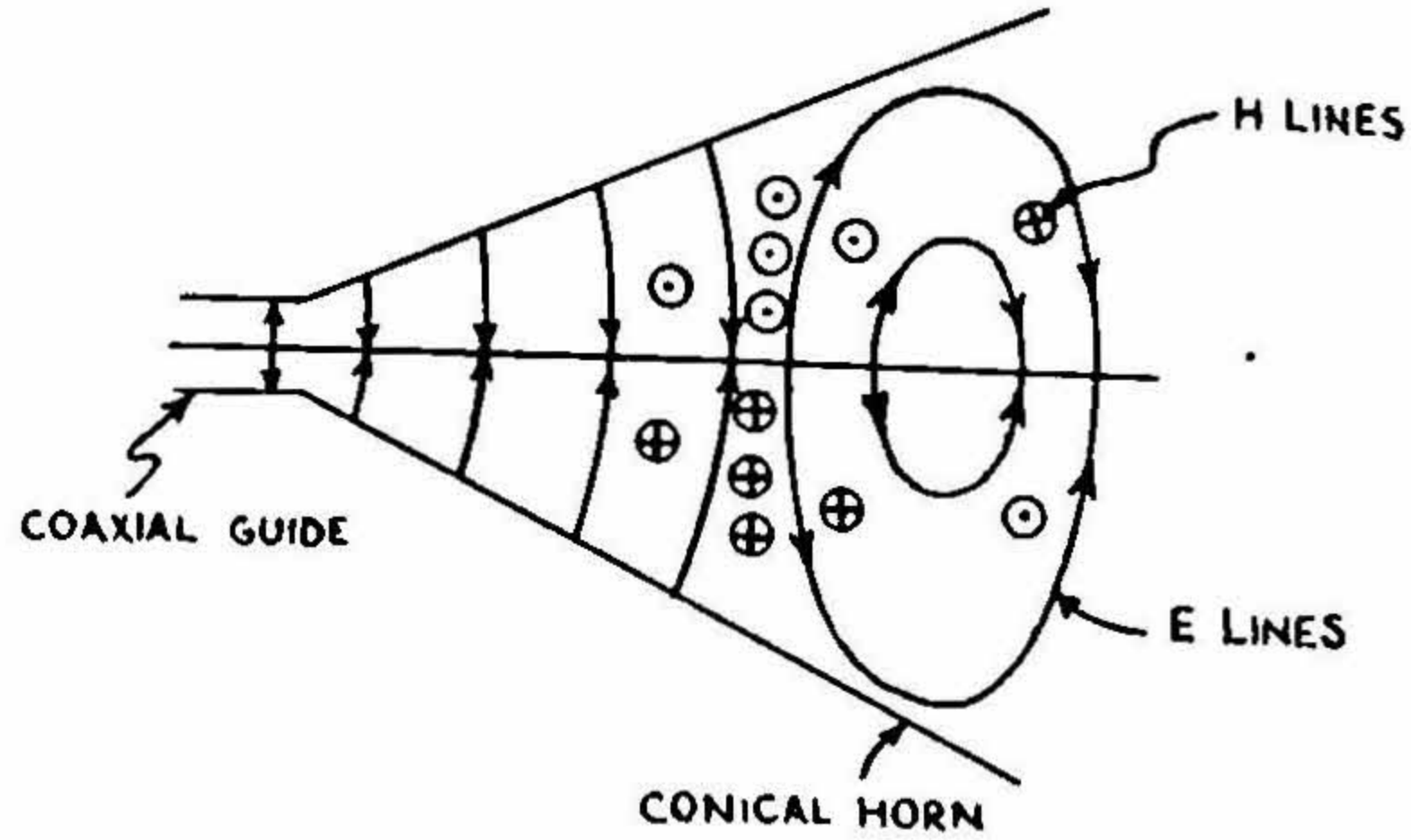
$$\begin{aligned}
 E_x &= \gamma_1^2 A J_0(\gamma_1 r) e^{-j\gamma x} \\
 E_r &= j\gamma\gamma_1 A J_1(\gamma_1 r) e^{-j\gamma x} \\
 H_\theta &= \frac{j\omega\epsilon\gamma_1}{c} A J_1(\gamma_1 r) e^{-j\gamma x}
 \end{aligned}
 \tag{14}$$

The Bessel function of the second kind has been omitted as it $\rightarrow -\infty$ as $r \rightarrow 0$. A rigorous analysis of the fields inside a conical horn of semi-infinite extent having a cylindrical conductor passing through the polar axis requires the use of two co-ordinate systems r, θ, ϕ and r, θ, x and hence both the sets of equations (13) and (14) are to be used. This makes the problem rather complicated. If, however, the cone aperture is large, there will be better similarity of the wave inside the horn and on the transmission line. But the use of r, θ, x co-ordinate requires a small flare angle, so that the region in the neighbourhood of the aperture may be considered as a cylinder surrounding the axial conductor. These two requirements necessitate the use of a long horn with small flare angle for achieving efficient launching. The field distribution in the launching system is shown in Fig. 4.

(ii) *Horn*.—The conical horn used for launching the surface wave has been designed by using the following formulæ and the design chart given by King (1950).

$$\begin{aligned}
 \frac{l}{\lambda} - \frac{L}{\lambda} &= 0.3 \\
 \frac{L}{\lambda} &\approx 0.3 (d/\lambda)^2
 \end{aligned}
 \tag{15}$$

The actual dimensions of the horn had to be changed slightly from optimum values due to practical reasons of construction. The dimensional sketches of the horn is shown in Fig. 5.



⊙ ⊕ Represent H Lines which are circularly symmetric with the Surface Wave Line.

FIG. 4. Field Distribution in the Launching Horn.

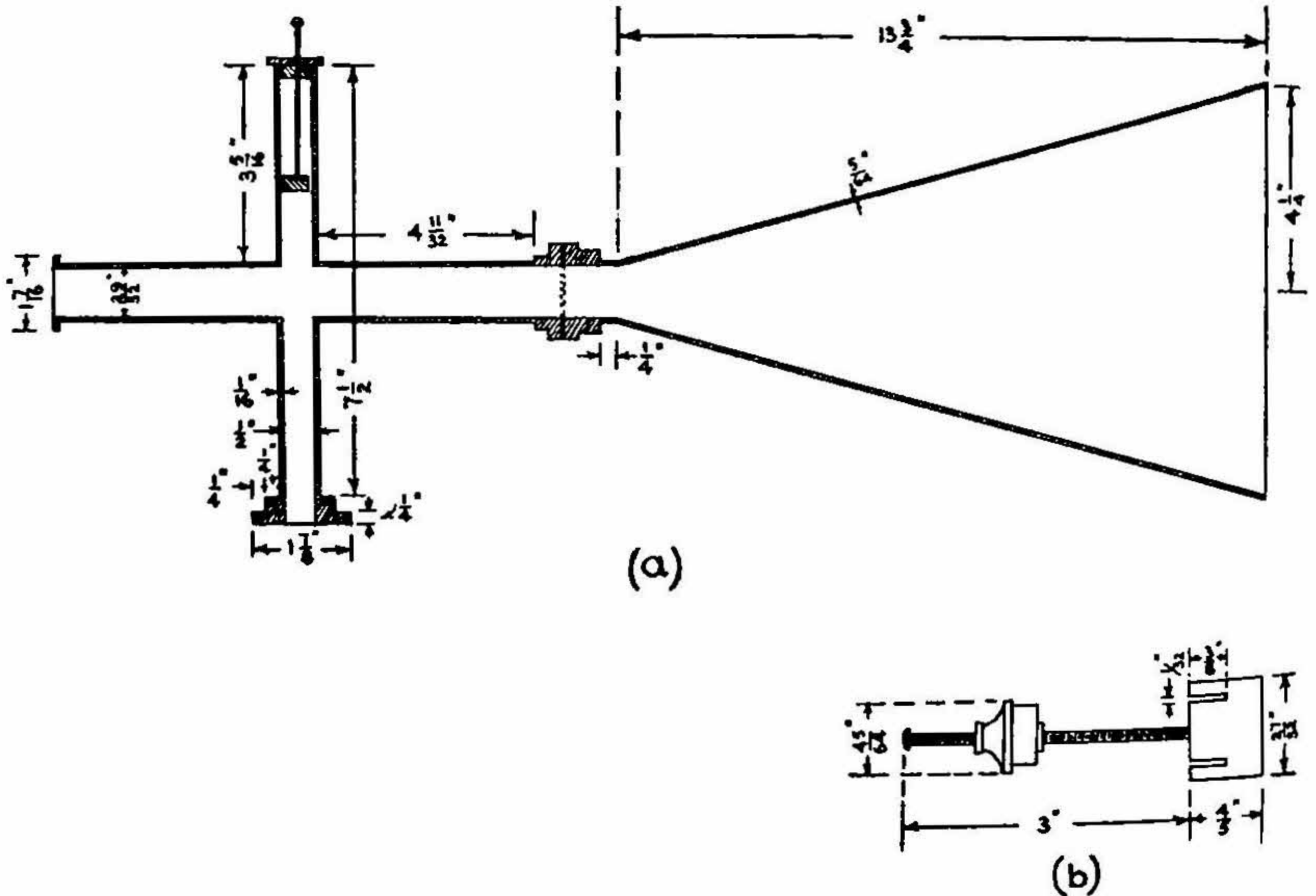


FIG. 5. Dimensional Sketches of (a) Conical Horn with Waveguide-transformer and (b) Plunger.

The absolute gain of the horn as measured by following the usual method (Cutler, etc., 1947) is 19.1 db. The E and H plane radiation characteristics of the horn were measured and the results are shown in Fig. 6 and Fig. 7. The half power beam widths are 10.0° and 8.5° for the E and H plane characteristics

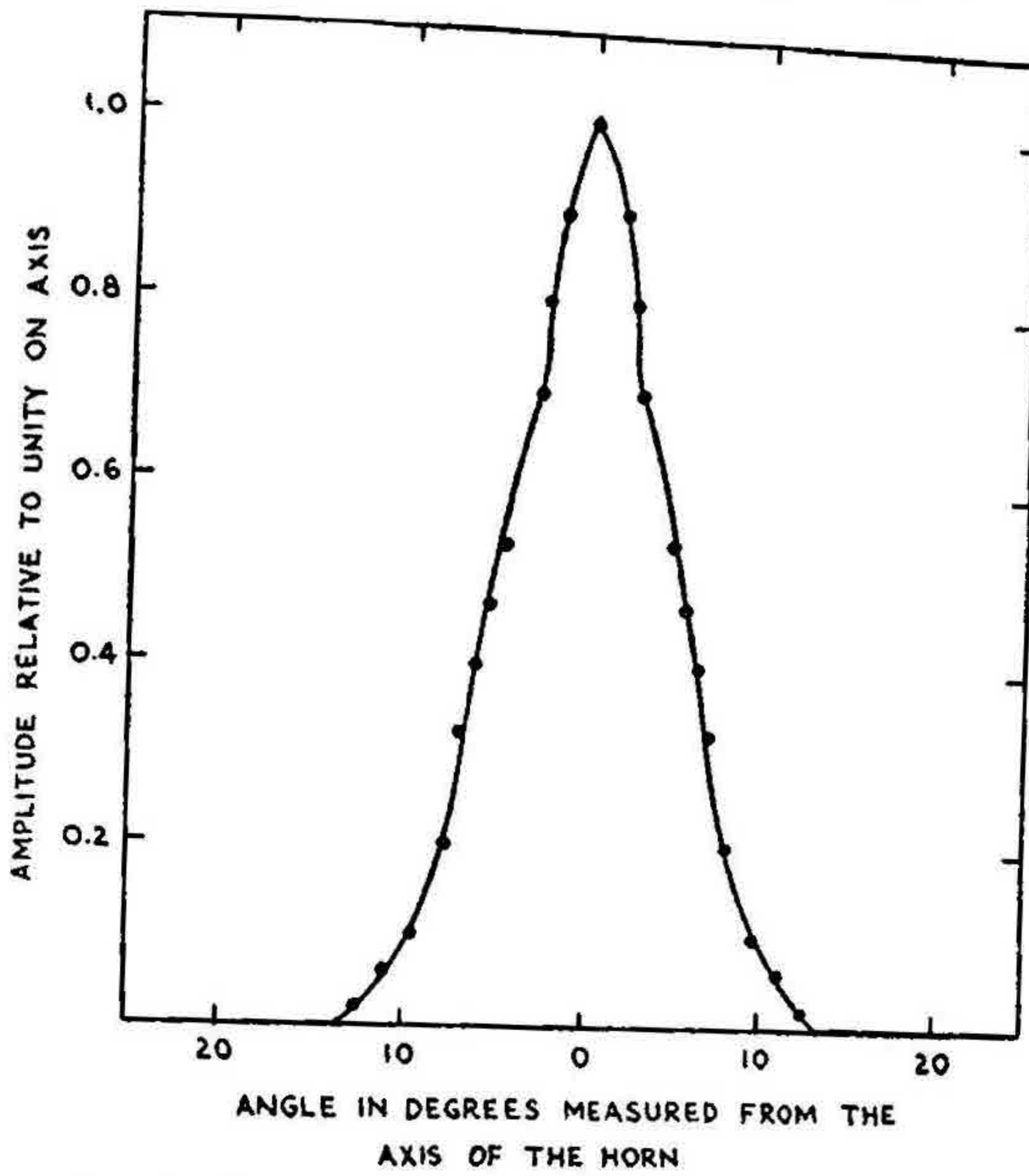


FIG. 6. Radiation Pattern of the Conical Horn E-Plane.

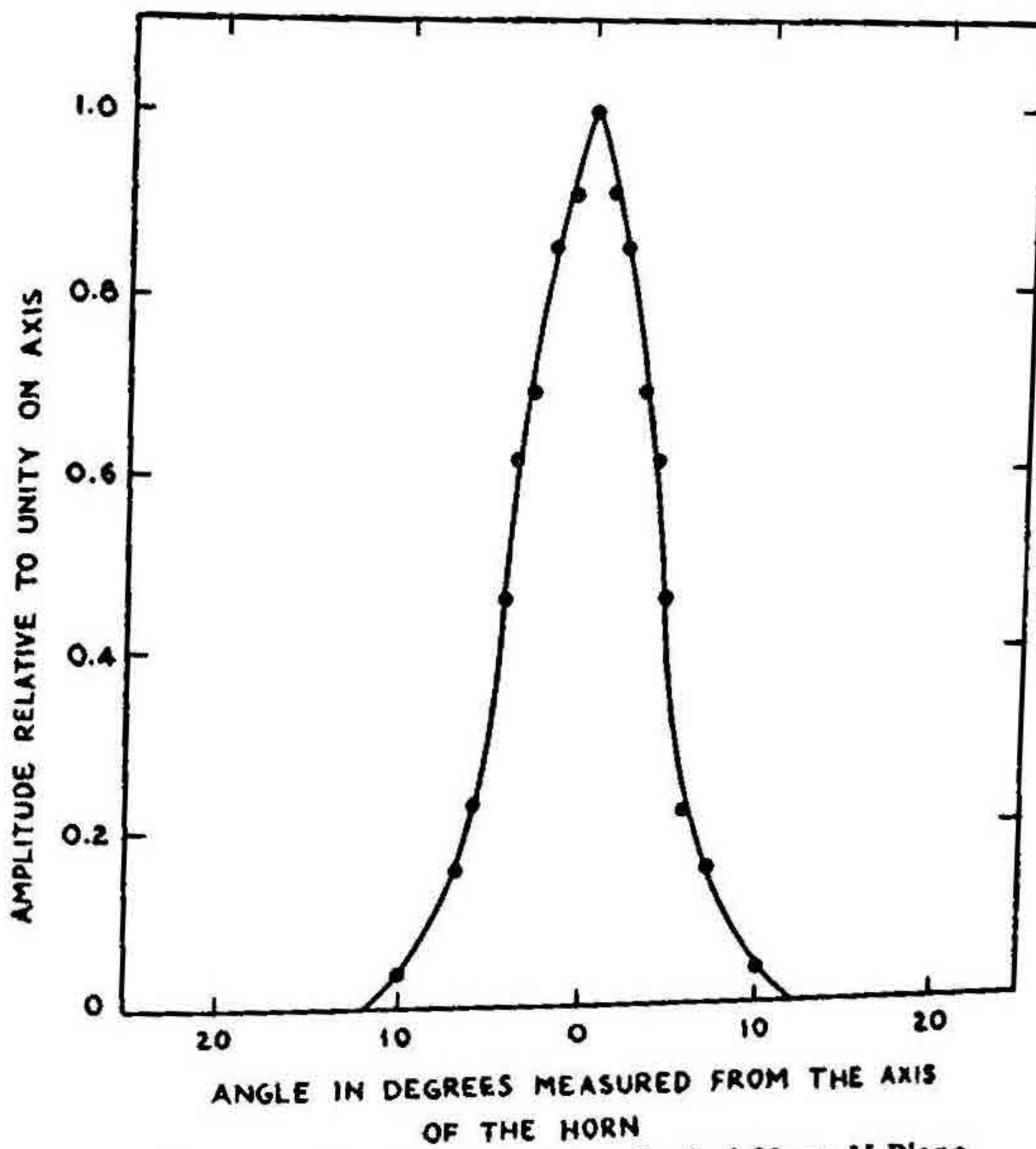


FIG. 7. Radiation Pattern of the Conical Horn H-Plane.

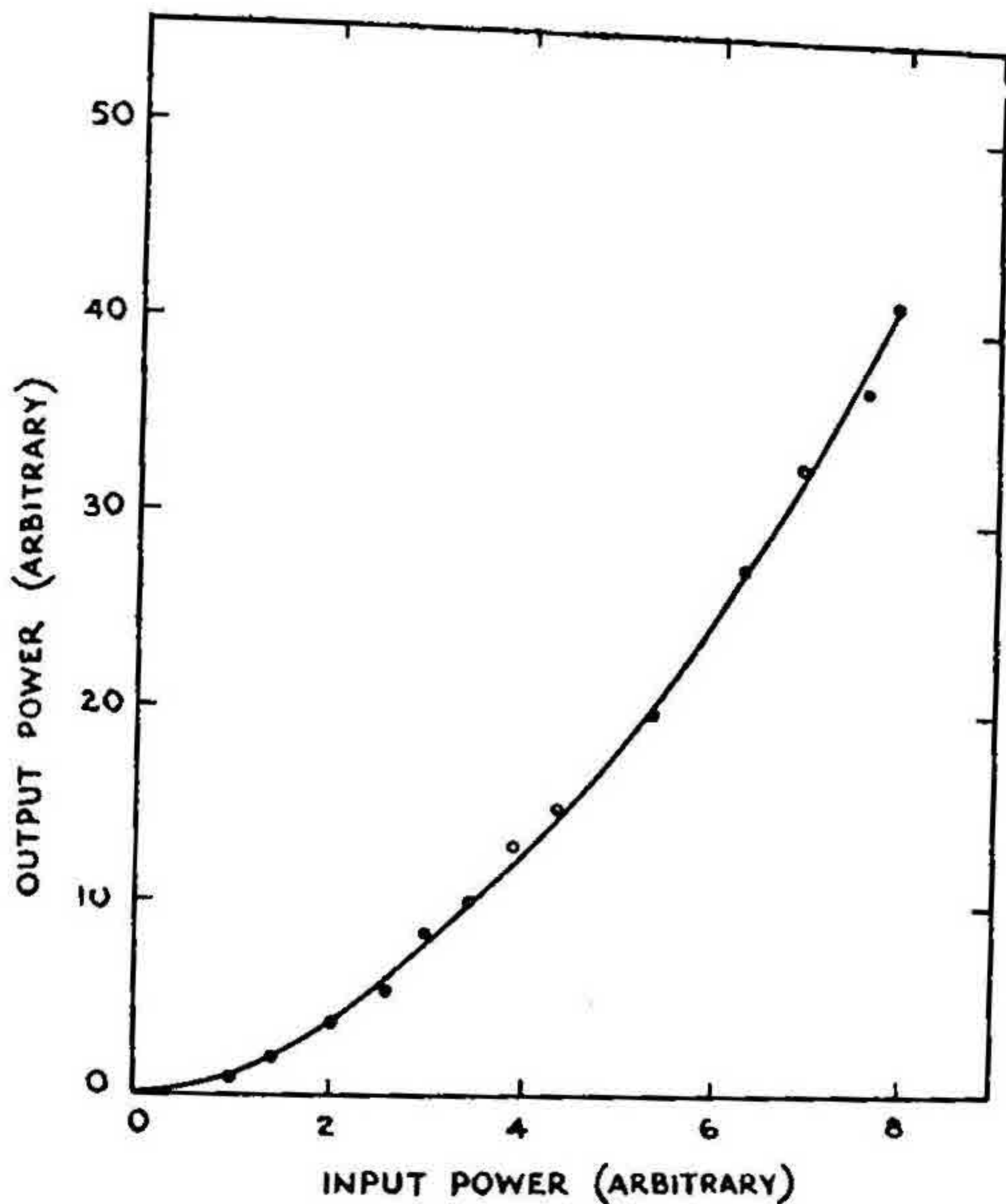


FIG. 9. Response Characteristic of Probe-Detector-Amplifier Combination.

In order to determine the direct interaction between the probe and the launching horn, the field picked up by the probe at different distances from the launching horn without the transmission line has been measured. Figure 10 shows the field strength vs. distance curves. It will be noticed that near the aperture of the horn, there is considerable fluctuations in the field strength with distance. This may be due to the following reasons. The wavefront inside the horn is spherical while on the transmission line it is plane. The horn aperture therefore causes a sharp discontinuity, giving rise thereby to higher order modes. So, in the neighbourhood of the aperture outside the horn, the surface wave mode is contaminated with other modes whose planes of polarisation are different. These complementary modes are rapidly damped out with distance. Hence, at larger distances, the exponential decay is an indication that a pure wave is existing. The other reason may be that due to the proximity of the probe to the horn, there occurs successive reflections. The reflected wave adding up with the forward wave at random phase is responsible for such wide departure from an exponential decay characteristic. In order to avoid the interaction between the probe and the launching horn, the radial field measurements have been done at a distance where the possibility of direct interaction is minimum.

(iv) *Mode transformer*.—A rectangular guide (RG-51/U) is excited in H_{01} mode from a klystron (2k39) by means of a co-axial adapter constructed for the

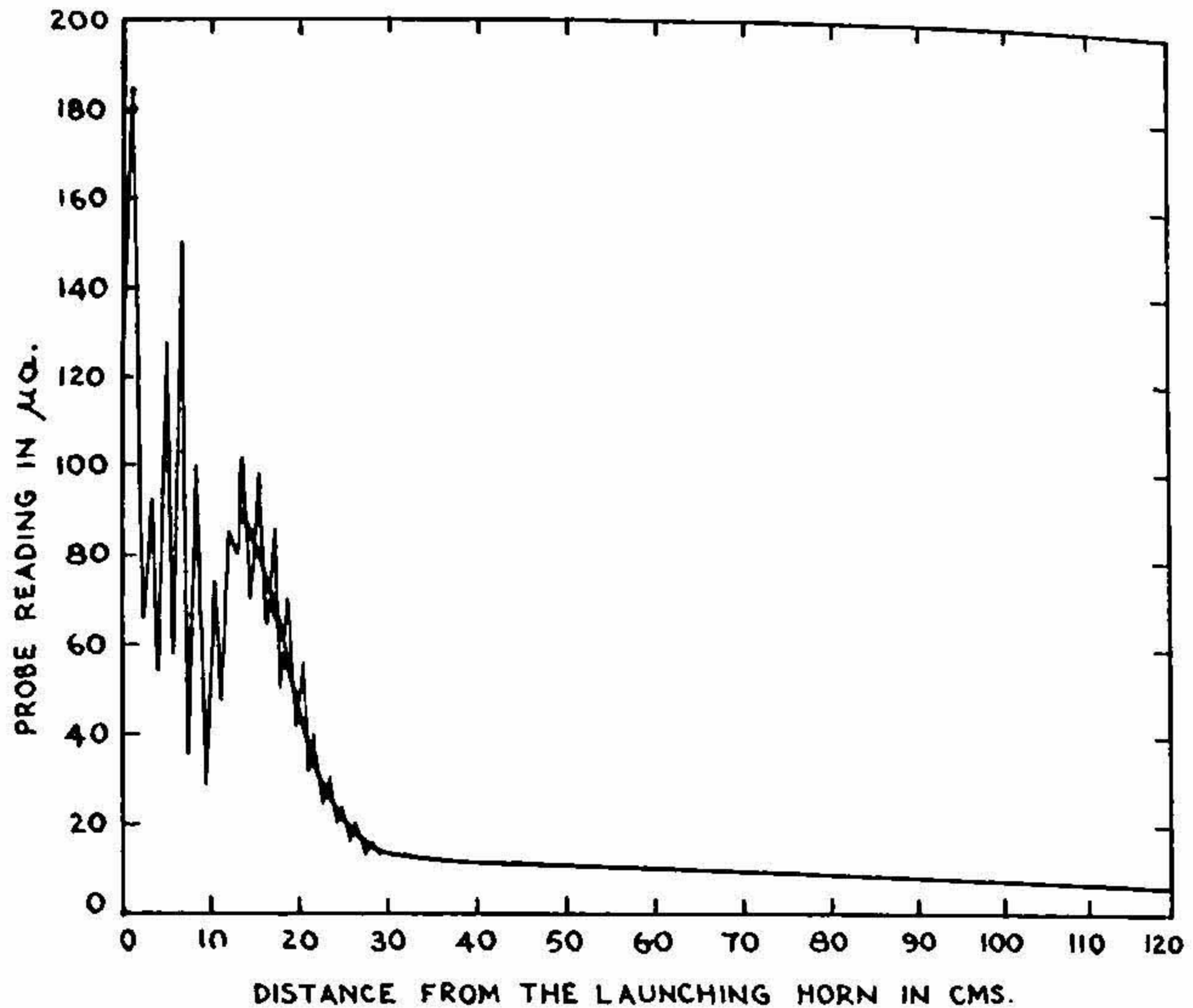
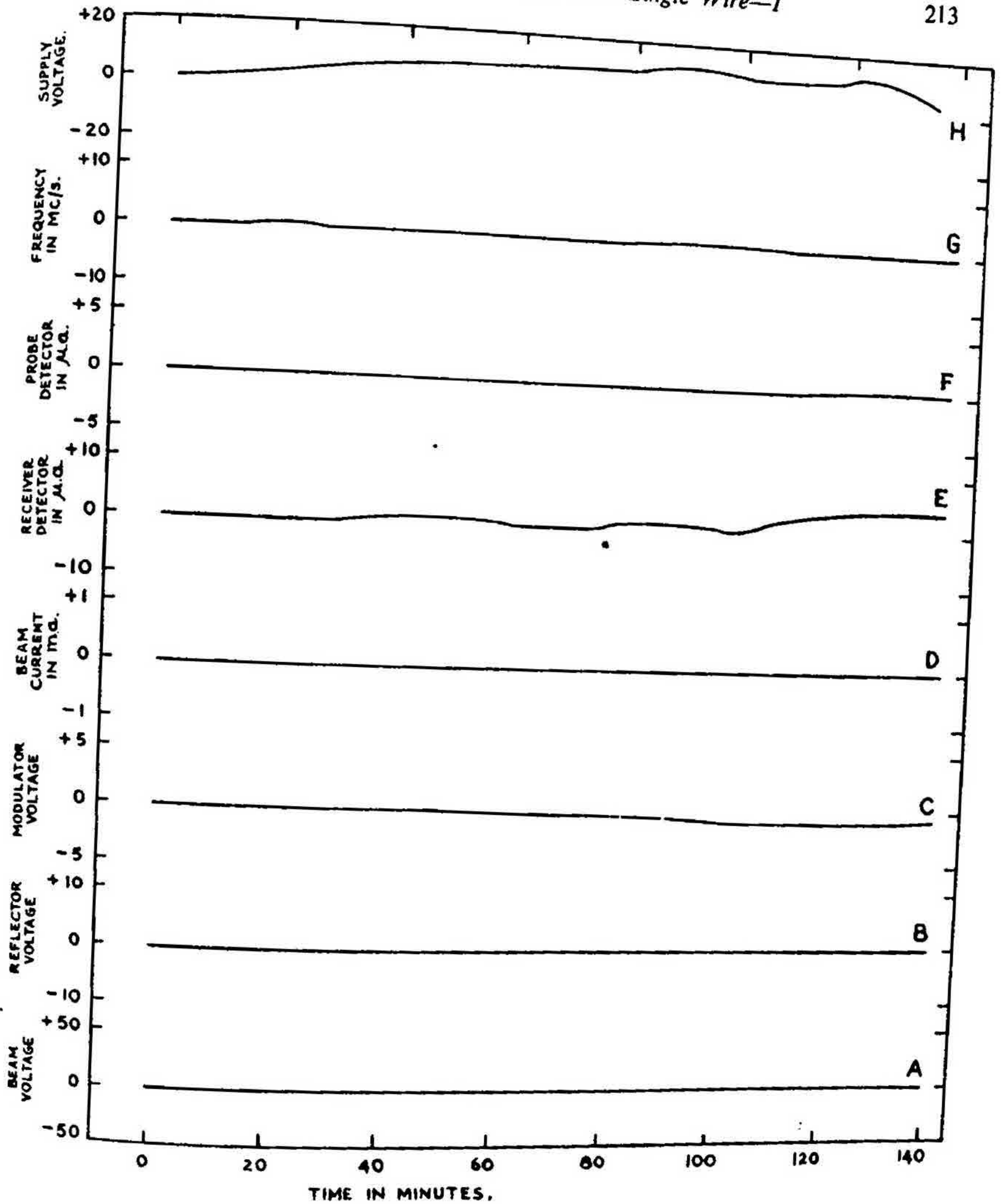


FIG. 10. Field Picked up by the Probe at Different Distances from the Launching Horn without Central Conductor.

purpose. The rectangular guide is connected at the broad faces to a cylindrical guide of inside diameter 0.91 inches. The launching horn is connected to one end of the cylindrical guide, the other end of which is terminated by a wooden plug. The other end of the rectangular guide is fitted with an adjustable plunger. A dimensional sketch of the mode transformer is shown along with the horn in Fig. 5.

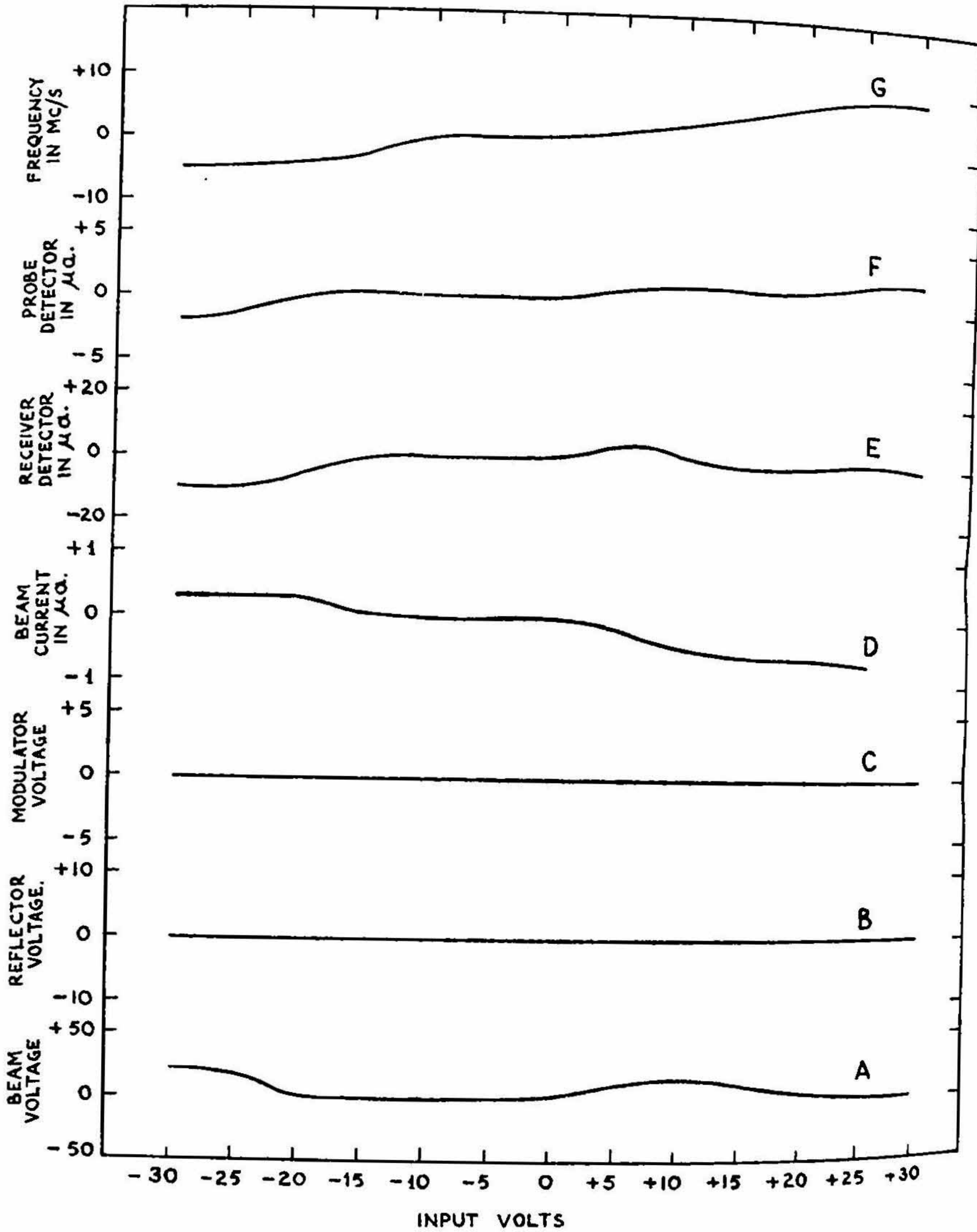
(v) *Surface wave transmission line.*—A single wire transmission line can support a non-radiating surface wave mode, due to its having finite conductivity which causes a reduction in phase velocity from the value of the free space velocity. It is the surface resistance of the wire which is mainly responsible for the establishment of non-radiating surface wave. Consequently, microwave frequencies are well suited for surface wave transmission. The conductivity loss however, increases with increasing frequency (Goubau, 1954). The radiation loss from the surface wave line depends upon the design of the launching device. It is intended to make a detailed study of the loss due to launching in a later paper. Theoretical calculations of the launching loss and the upper frequency limit of use for surface wave transmission are lacking. The transmission line used in the present experiment is 12 s.w.g. bare copper wire. A comparative study for different gauges of wire will be reported in a later paper.

(vi) *Receiver.*—The receiving end consists of a similar cone through which the surface wave transmission line passes. The cone is connected to a detecting



A - BEAM VOLTAGE D - BEAM CURRENT. G - FREQUENCY
 B - REFLECTOR VOLTAGE. E - RECEIVER DETECTOR H - SUPPLY VOLTAGE
 C - MODULATOR VOLTAGE F - PROBE DETECTOR

FIG. 11. Stability Characteristics of the System with respect to Time.
 The Variations in Different Quantities are Plotted.



- | | |
|-----------------------|-----------------------|
| A - BEAM VOLTAGE | E - RECEIVER DETECTOR |
| B - REFLECTOR VOLTAGE | F - PROBE DETECTOR |
| C - MODULATOR VOLTAGE | G - FREQUENCY |
| D - BEAM CURRENT | |

FIG. 12. Stability Characteristics of the System with respect to the Variations in Input Voltage. Only the Variations in Different Quantities are Plotted.

section through a mode transformer as described above. The detecting section is connected to an amplifier by means of a co-axial cable. The detector amplifier is used to monitor the stability of klystron output. A frequencymeter 558-A PRD type is connected at the receiving end for frequency monitoring.

(vii) *Power supply and modulator unit.*—The power is fed to the system at 9322.2 mc./s. from a 2k39 klystron. The power supply and modulator unit for the klystron have been constructed by using the same circuit as that of Mark SX-12 (Montgomery, 1947). The klystron is operated at a reflector voltage of -530 volts, beam voltage of 1200 volts and a beam current of 27 m.a. As the rate of frequency deviation is lowest in the high reflector voltage modes and the power output is also high, the reflector is operated at a high voltage. The stability characteristics of the system with respect to time and supply voltage variations have been determined and are presented in Figs. 11 and 12, where only the variations in different quantities have been plotted. It is to be noticed from Fig. 11 that the frequency of the klystron varies by ± 0.15 mc./s. which does not produce any significant change in the power output of the klystron as found from the mode curve and frequency deviation curve of the klystron. A bolometer bridge for monitoring the power output of the klystron is under construction.

The modulator unit consists of a multivibrator followed by a clipper and shaper. The modulator voltage output is superimposed on the d.c. reflector voltage. In order to have minimum frequency modulation, particular care has been taken to adjust the shaper and clipper to ensure that the leading and the trailing edges of the square wave are as steep as possible. A photograph of the square wave used for modulation is shown in Fig. 13. The amplitude of the modulated voltage has been adjusted in relation to the particular mode of the klystron so that the modulated wave switches the klystron power output on and off the mode, thereby ensuring minimum of frequency modulation.

(viii) *Detector amplifier.*—The detector amplifier consists of six stages of amplification having a twin-tee network in the fourth stage. The operating gain of the amplifier is 70 db. The selectivity, phase characteristics, etc., of the amplifier have been reported elsewhere by Chatterjee, etc. (1954). The linearity characteristics of the detector and amplifier combination is shown in Fig. 14.

(ix) *Experimental set-up.*—The block schematic in Fig. 15 shows the experimental set-up. Figure 16 shows the photograph of the transmitting end with launching horn and power supply system. The photograph of the receiving end is shown in Fig. 17. Figure 18 shows the actual arrangement with probe-detector-amplifier mounted on a rail used for exploring field distribution.

(x) *Interaction between horns.*—When the receiving horn is introduced into the far end of the surface wave line, it gives rise to a scattered wave. A part of this scattered wave is intercepted by the launching horn which in turn acts as a source of scattering. The scattered wave is partly absorbed and partly scattered by the receiving horn. This multiple scattering and absorption due to the interaction gives rise to a standing wave pattern in the space between the two horns.

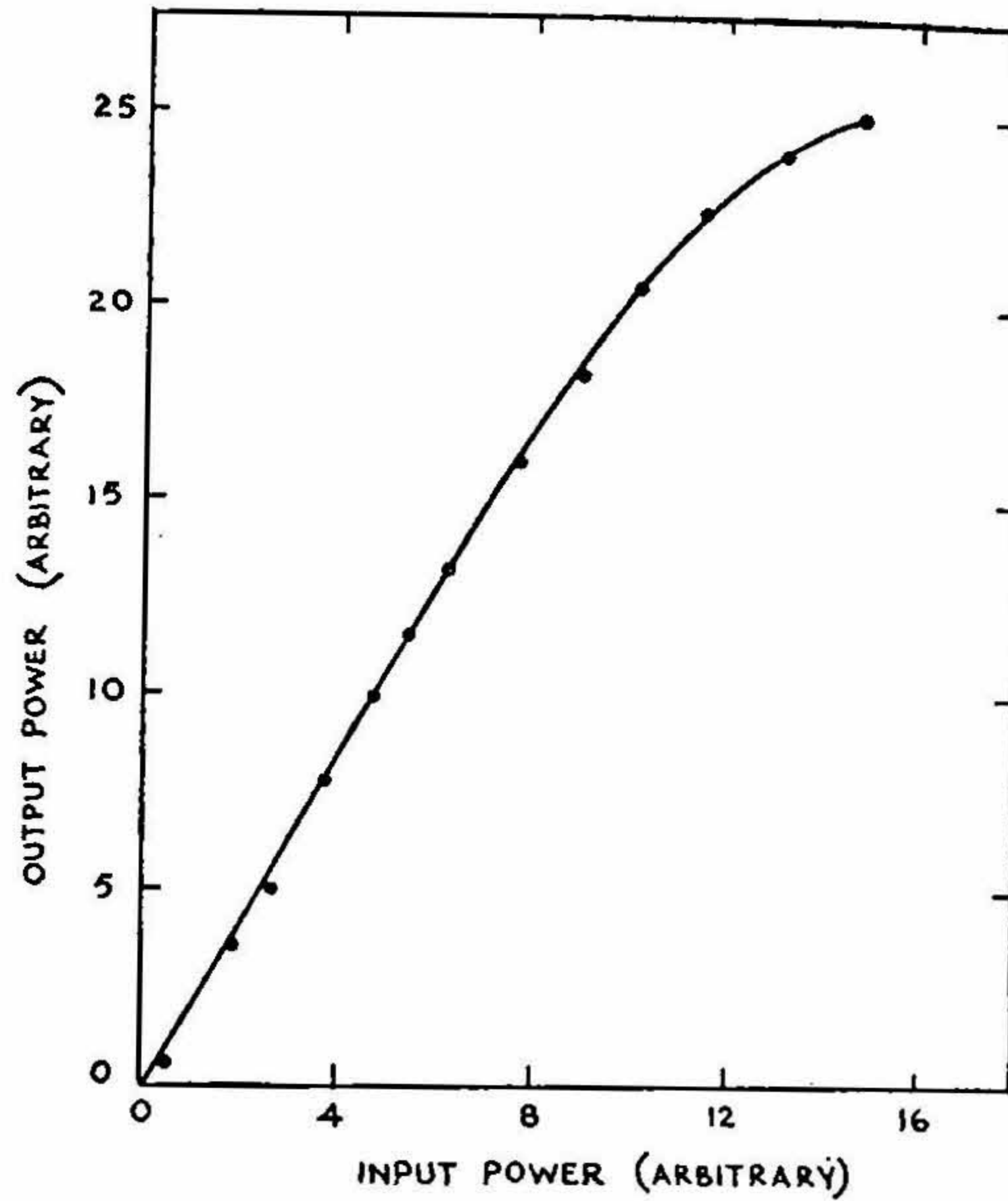


FIG. 14. Linearity Characteristic of Detector-Amplifier.

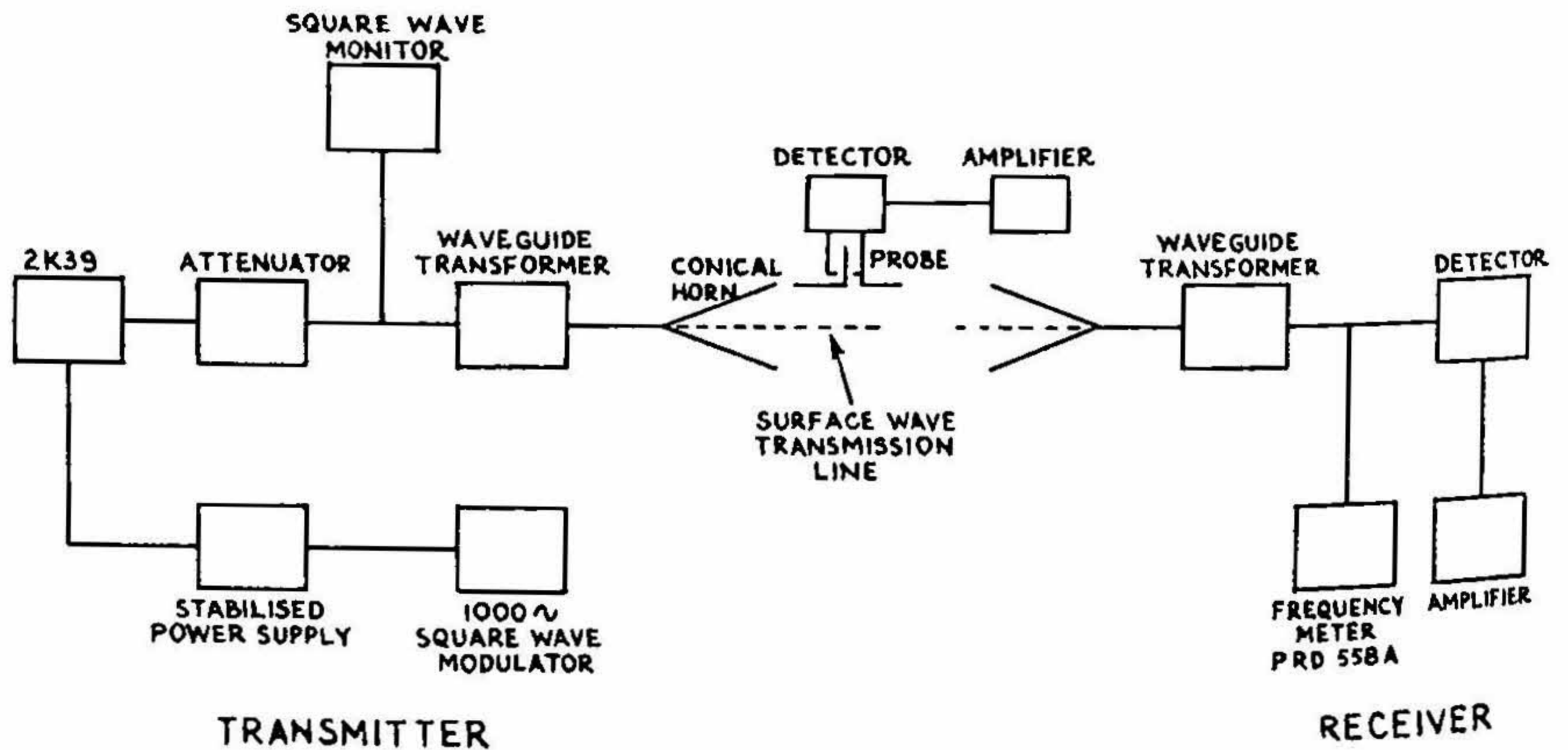


FIG. 15. Block Schematic Diagram of the Experimental set-up used for Surface-Wave Propagation.

The amplitude of the wave received by a horn due to the process of single scattering decreases inversely as the square of the distance and due to multiple scattering

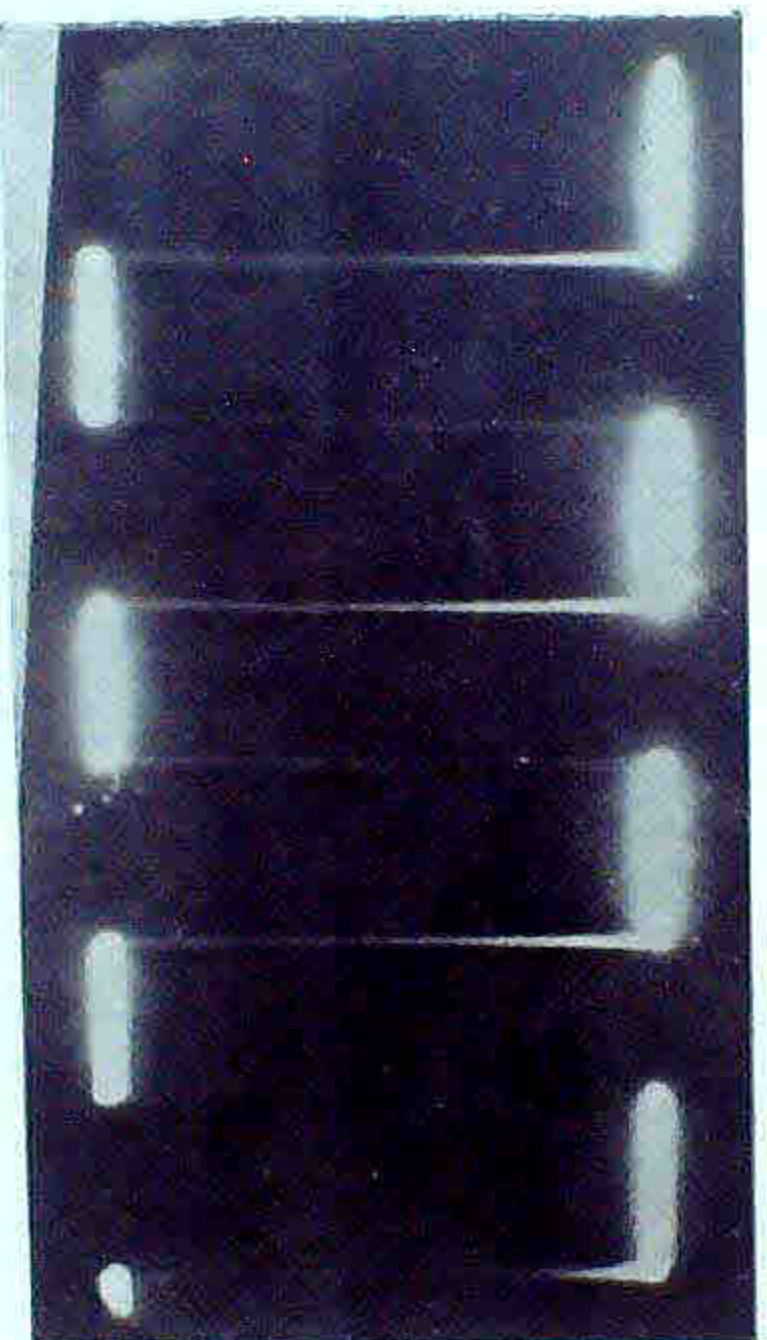


FIG. 13. Photograph of the Square Wave.

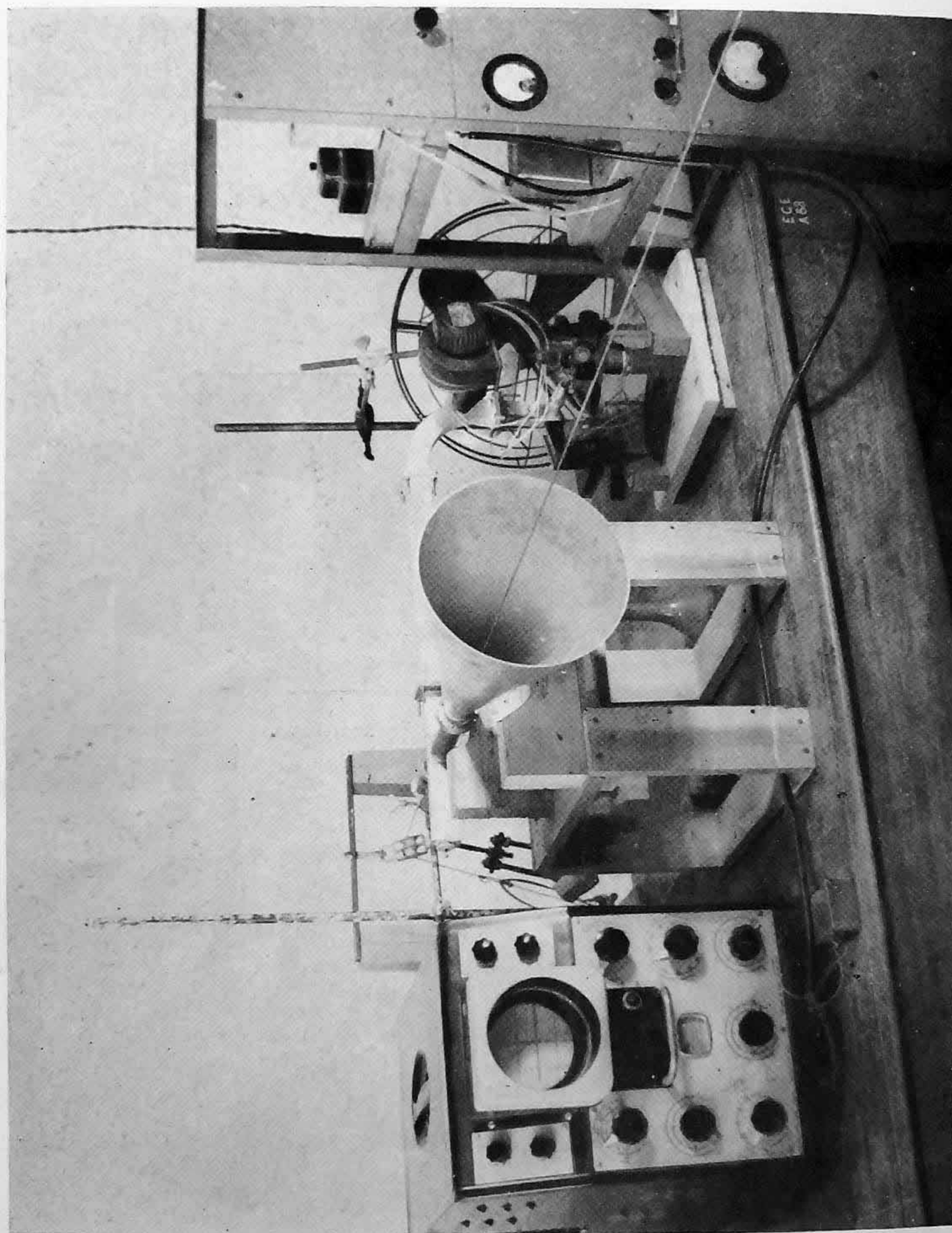


FIG. 16. Photograph of the Launching System.

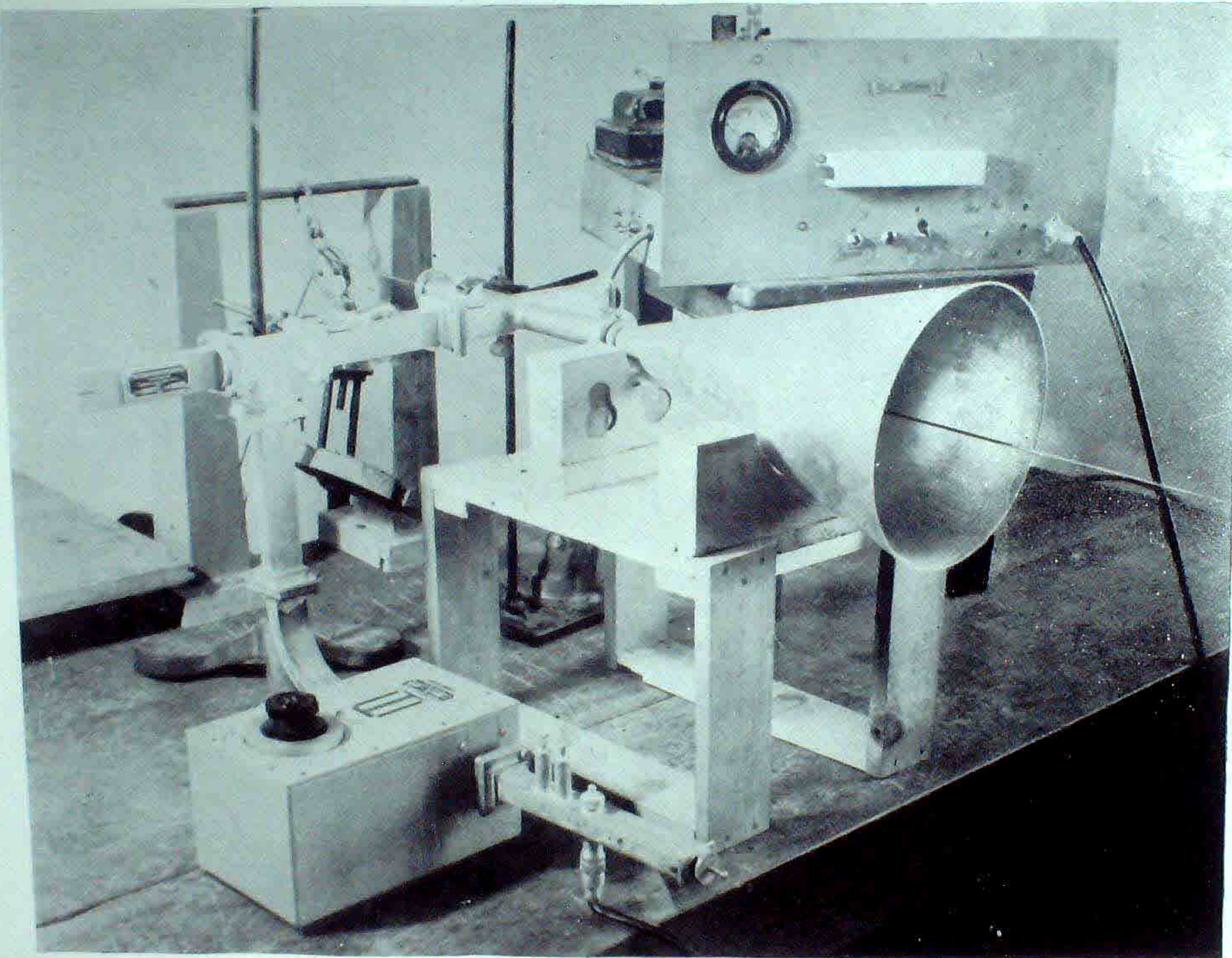


FIG. 17. Photograph of the Receiving End.

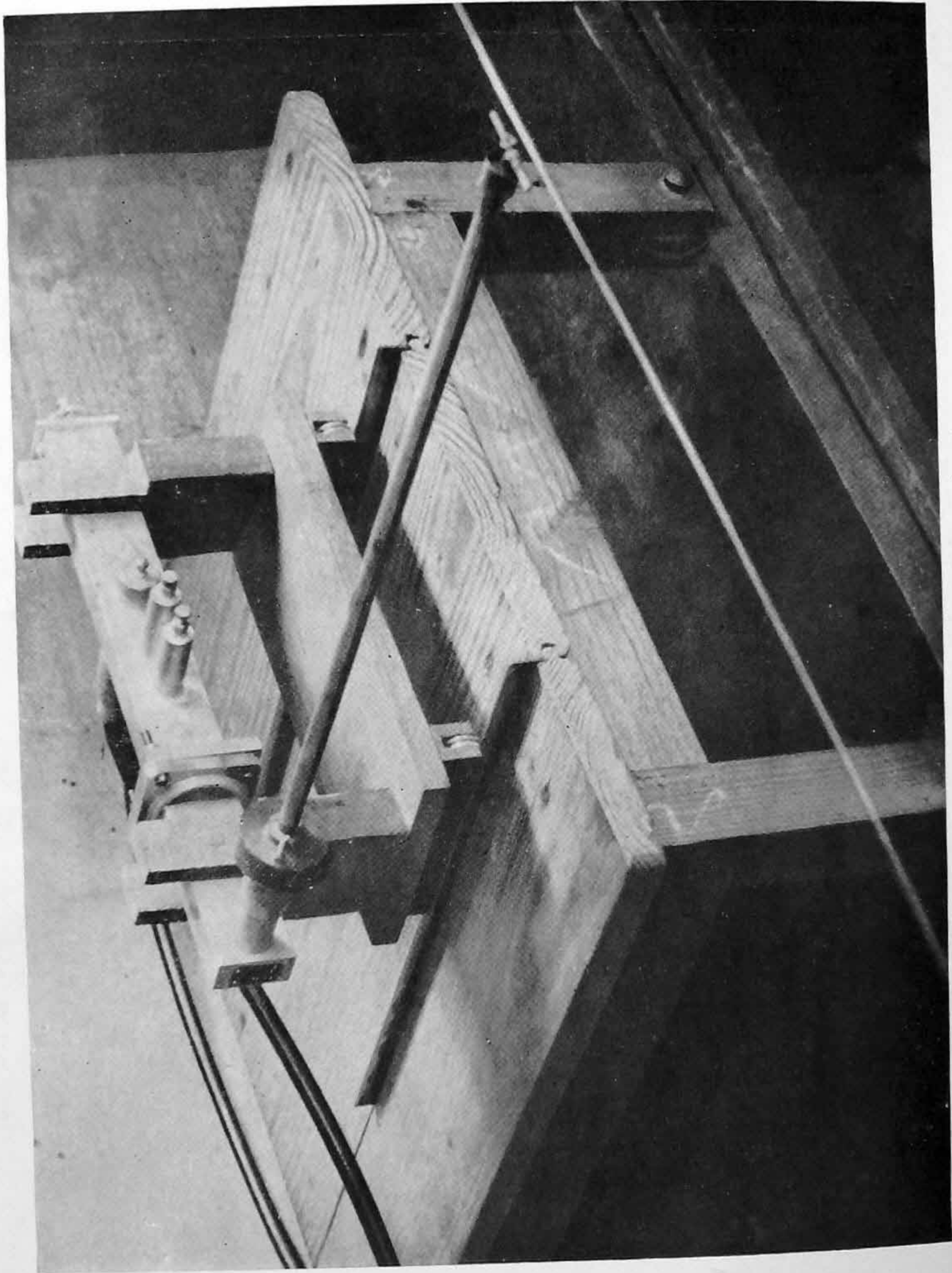


FIG. 18. Photograph of the Probe-detector.

decreases inversely as the fourth power of the distance between the two horns. So, at a large distance from the launching horn, the interaction practically vanishes. In order to determine the minimum distance at which the interaction between the two horns vanishes, the energy received by the receiving horn has been measured as a function of the distance from the launching horn. The result is presented in Fig. 19. The measurements have been done upto a distance of about 7 metres

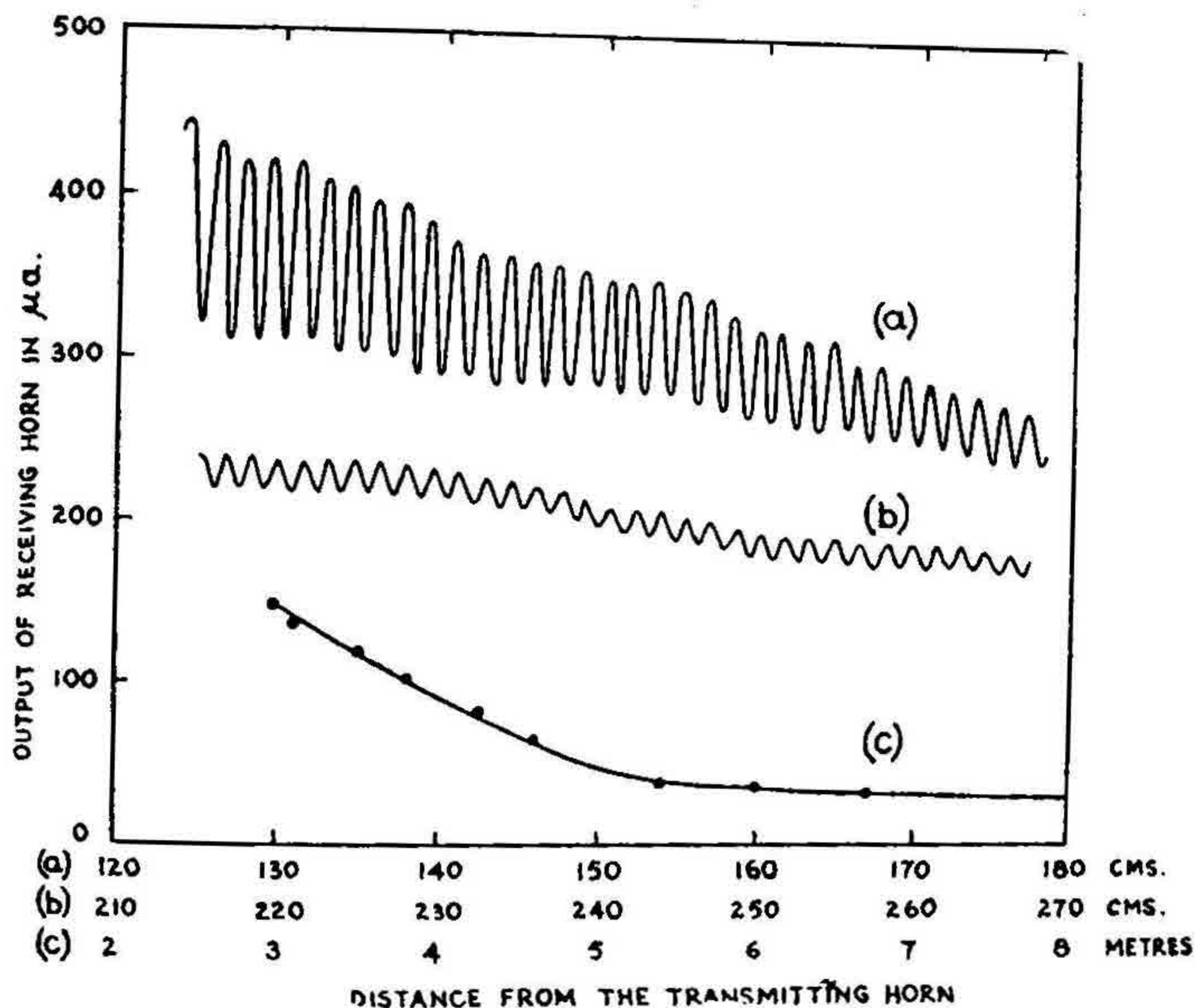


FIG. 19. Interaction between Horns.

- (a) Receiving Horn Near the Launching End.
- (b) Receiving Horn Near the Middle of the Transmission Line.
- (c) Receiving Horn Near the End of the Transmission Line.

from a distance of about 1 metre from the launching horn. It is observed from Fig. 19 (a) that the interaction is quite significant upto a distance of about 3 metres. After this distance, the exponential decay shows negligible interaction. The distance between the transmitting and receiving horn in the present experiment is about 8 metres. The distance could not be further increased due to lack of space.

(xi) *Effect of termination.*—Before making any measurement of radial field spread it is necessary that both the launching and the receiving ends are matched to the surface wave line. The initial matching is done by means of the waveguide plunger at both ends. The probe was moved on a rail parallel to the line and the standing wave pattern observed showed the necessity of further matching. This has been done by using tapered wooden terminations to absorb the energy of the

wave on the wire at the receiving end. The standing wave ratio along the line was checked to ensure that there is no appreciable reflections. Some of the results of measurements are reported in Fig. 20. The dimensional sketch of the terminations is shown in Fig. 21. The v.s.w.r. without termination is 10.28. The v.s.w.r. with terminations (*b*) and (*a*) are 1.65 and 1.02 respectively. The latter

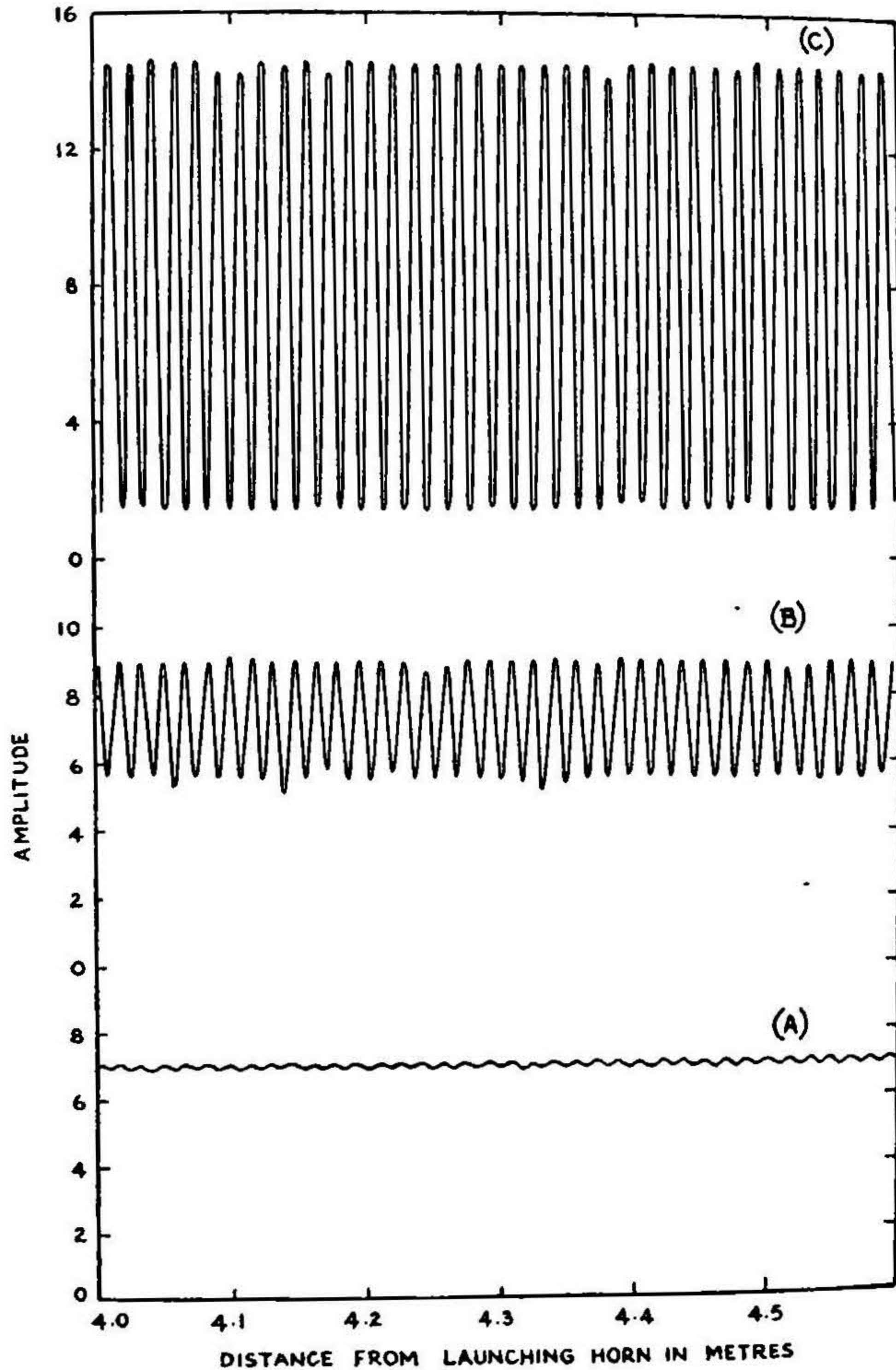


FIG. 20. Effect of Terminations on Standing Wave.
 (A)—Termination (*a*), (B)—Termination (*b*), (C)—Without Termination.

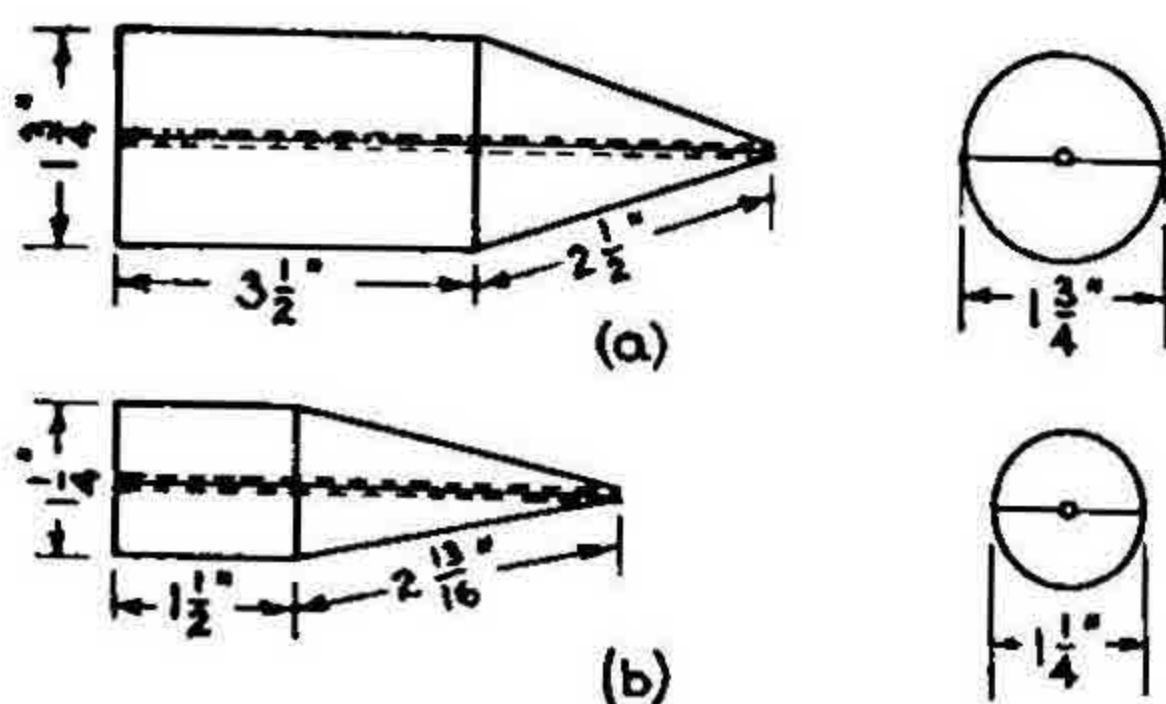


FIG. 21. Dimensional Sketches of Terminations.

value almost ensures the absence of any reflection. However, further work to select a suitable termination so as to ensure a perfect matched condition is under progress.

(xii) *Extension of field in the radial direction.*—The decay of field strength with distance from the wire in the radial direction as obtained experimentally is

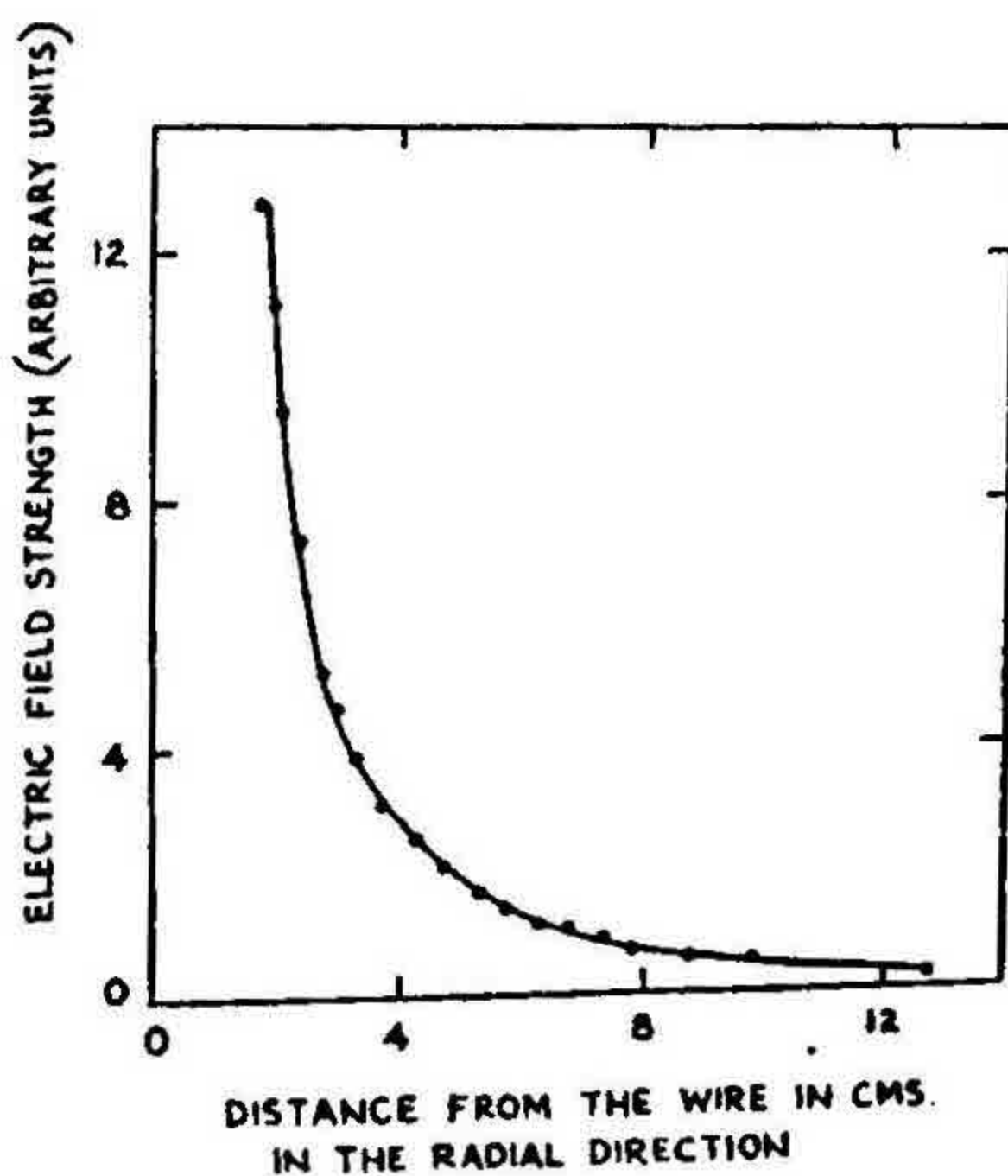


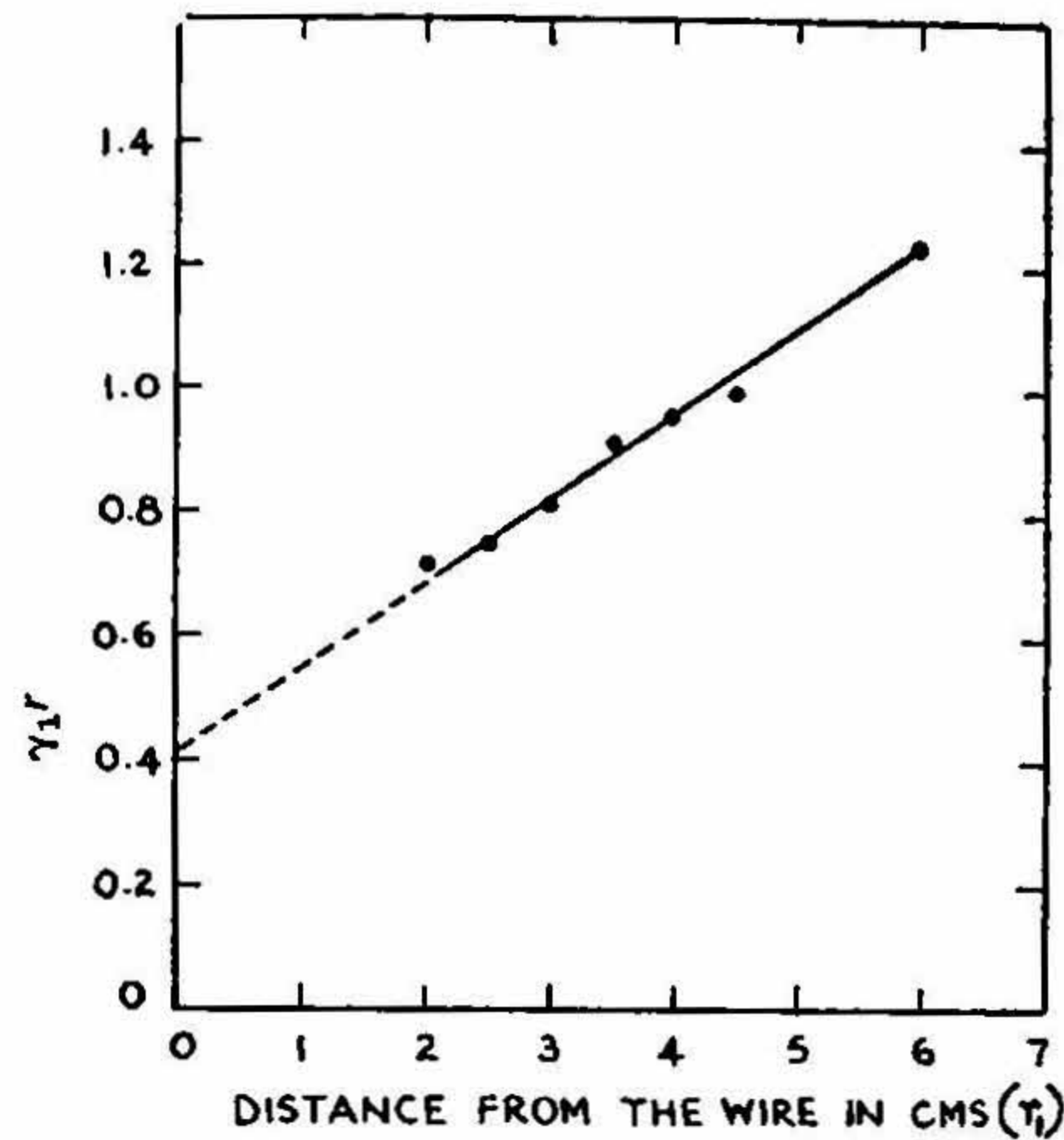
FIG. 22. Variation of Radial Electric Field with Radial Distance.

shown in Fig. 22. The curve gives the ratio

$$f_n(\gamma_1 r) = \frac{H_1^{(1)}(j\gamma_1 r_2)}{H_1^{(1)}(j\gamma_1 r_1)} \quad (16)$$

for different values of r_1 with the values for the identifying constant $n = r_2/r_1 = 2.0$. Burlow and Karbowskiak (1953) have plotted the identifying curve $f_n(\gamma_1 r)$ vs. $\gamma_1 r$. $\gamma_1 r$ corresponding to $f_n(\gamma_1 r)$ given by equation (16) for different values of r_1 is found and plotted in Fig. 23. The slope of the curve gives the real part of γ_1 ,

i.e., α_1 which is the experimental value of the radial decay coefficient. The value obtained for α_1 is 14.0 m^{-1} . The linearity of the decay coefficient curve (Fig. 23) indicates the purity of surface wave. The field strength decay curve is better



MEASURED SLOPE = 0.140 cm^{-1} DECAY COEFF. (α) = 14.0 m^{-1}

FIG. 23. Decay Coefficient Curve.

understood from Fig. 24. The field strengths at different distances have been plotted with respect to the field strength that could be measured at the closest distance between the wire and the centre of the dipole which is 1.75 cm .

(xiii) *Energy distribution in the radial direction.*—The theoretical energy distribution curve has been plotted with the help of equations 10 to 12 for a 12 s.w.g. bare copper wire having a smooth untarnished surface. The experimental energy distribution curve has been plotted in the following way. The value of γ_1 is as follows (Burlow, 1952).

$$\gamma_1 = \frac{1.12 |\xi|^{1/2}}{a} e^{j \left(\frac{\zeta + \pi}{2} \right)} = \alpha_1 - j\beta_1 \quad (17)$$

where,

$$\zeta = -\frac{\pi}{4} \left[1 - \frac{1}{1 + \ln |\xi|} \right] \quad (18)$$

Taking the real part of γ_1 from equation (17) and using equation (18), the value of α_1 is obtained as follows:—

$$\alpha_1 = \frac{1.12 |\xi|^{1/2}}{a} \sin \frac{\pi}{8} \left[1 - \frac{1}{1 + \ln |\xi|} \right] \quad (19)$$

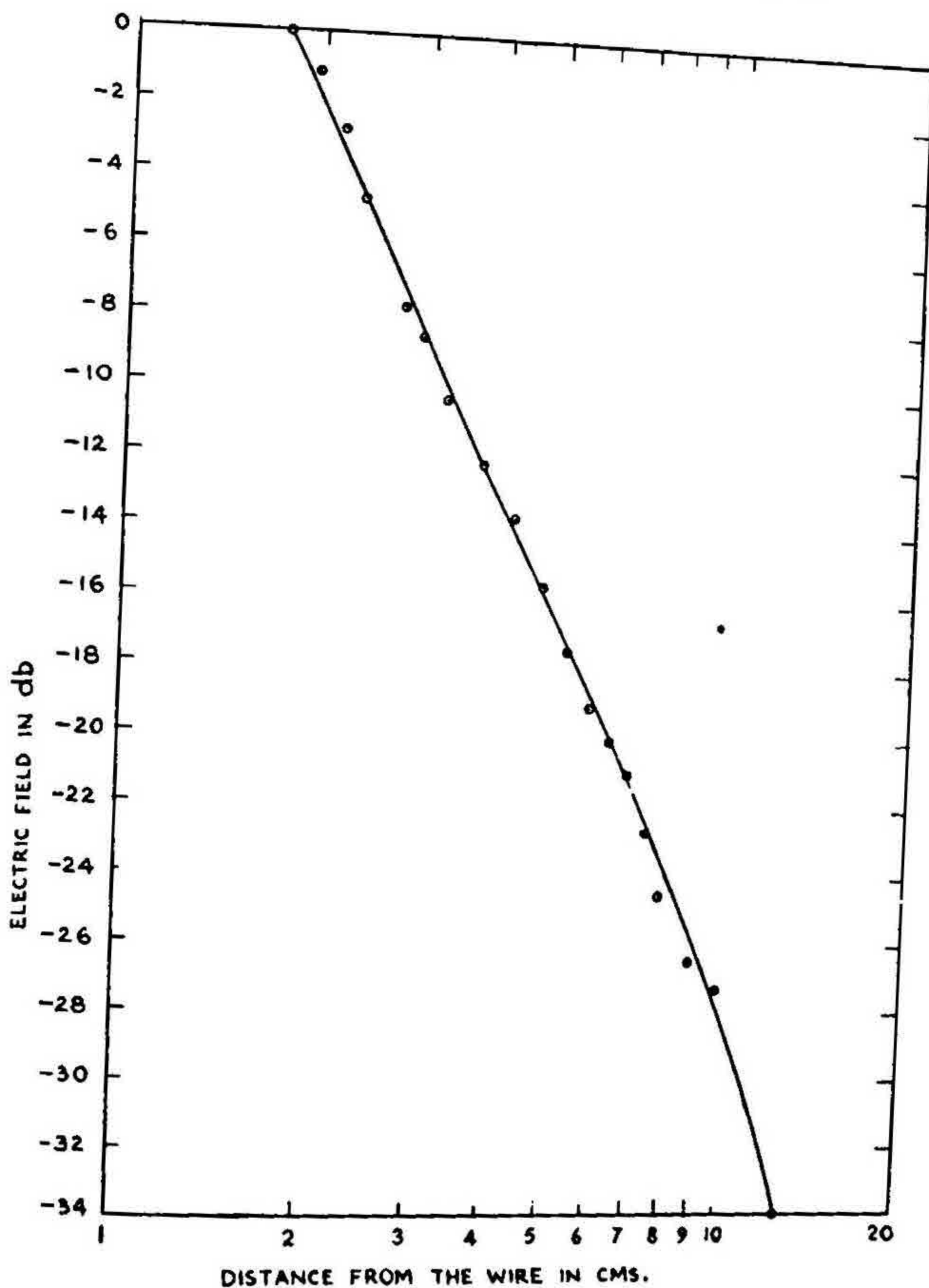


FIG. 24. Field Strength Decay Curve.

The experimental value of $\alpha_1 = 0.140 \text{ cm.}^{-1}$; the corresponding value of $|\xi|$ obtained from equation (19) is $\xi = 1.25 \times 10^{-5}$; whereas, the value of $|\xi|$ obtained from equation (12) is $\xi = 2.85 \times 10^{-6}$. The experimental value of ξ is substituted in equation (10) and the percentages of power flow at different distances have been calculated and plotted in Fig. 3.

The following table gives comparative values of percentages of power flow within areas enclosed by different radial distances from the wire as obtained from theory and experiment.

TABLE I
Comparative values of percentages of power flow

Percentages of power flow	Theoretical values of radial distances in cm.	Experimental values of radial distances in cm.
25	0.5	0.5
40	1.3	0.8
50	2.5	1.6
75	10.8	6.5
90	26.5	14.0

It is evident from the above table that the field has shrunk more than predicted by theory. The departure of the experimental results from the theoretical is considered to be due to following reasons. The theoretical power flow distribution curve has been calculated by taking $\xi = 2.85 \times 10^{-6}$, which is obtained from the theoretical value of $|\eta|$. The value of $|\eta|$ has been calculated by considering the surface of the conductor as perfectly smooth and taking the conductivity to be equal to the bulk conductivity of copper. But, in practice, the natural surface roughness combined with the usual oxide coating due to the surface being exposed to air is responsible for decreasing the value of surface conductivity. Consequently, the decay factor α_1 increases in value several times over the value which would be found if the surface would conform to the theoretical condition. The increase of α_1 tends to lower the phase velocity more than what is expected in the case of copper conductor having a smooth surface. Hence there would be greater shrinkage of field than the theoretical value.

(xiv) *Surface conductivity of metals.*—The relation between ξ , η and σ are as follows:—

$$|\xi| \ln |\xi| = -|\eta| \quad (11)$$

$$|\eta| = \frac{24.6 \times 10^{-14}}{\sqrt{\sigma}} af^{3/2} \quad (20)$$

The value of $|\eta|$ is 14.11×10^{-5} compared to $|\eta| = 3.6 \times 10^{-5}$ obtained from equation (12). From equation (20), $\sigma = 3.75 \times 10^{-6}$ mho/metre as compared to the bulk conductivity $\sigma = 5.7 \times 10^{-7}$ mho/metre. The surface roughness and the oxide coating are comparable to the skin depth. Therefore, σ found by above calculation is the surface conductivity under practical conditions. This is the conductivity with which we are interested, rather than bulk conductivity in microwave work. This method involving the experimental determination of the decay

factor may therefore be used to determine the surface conductivity of metals in the form of wire.

REFERENCES

- Zenneck, J. .. *Ann. d. Phys.*, 1907, 23, 846.
- Sommerfeld, A. .. *Ibid.*, 1909, 28, 665; *ibid.*, 1926, 81, 1135.
- Weyl, H. .. *Ibid.*, 1919, 60, 481.
- Rolf, B. .. *Proc. I.R.E.*, 1930, 18, 391.
- Norton, K. A. .. *Nature*, 1935, 135, 954.
- Burrows, C. R. .. *Ibid.*, 1936, 138, 284.
- Kahan, T. and Eckart, G. .. *Phys. Rev.*, 1949, 76, 406.
- Bowkamp, C. J. .. *Ibid.*, 1950, 80, 294.
- Wise, W. H. .. *B.S.T.J.*, 1937, 16, 35.
- Rice, S. O. .. *Ibid.*, 1937, 16, 101.
- Burrows, C. R. .. *Proc. I.R.E.*, 1937, 25, 219.
- Sommerfeld, A. .. *Ann. d. Phys. u. Chem.*, 1899, 67, 233.
- Goubau, G. .. *Jour. Appl. Phys.*, 1950, 21, 1119.
- Stratton, J. A. .. *Electromagnetic Theory*, 1941, 526, Published by McGraw Hill Book Co.
- Hondros, D. .. *Ann. d. Phys.*, 1909, 30, 905.
- Sommerfeld, A. .. *Ibid.*, 1904, 15, 673.
- Burlow, H. M. and Cullen, A. L. .. *Proc. I.E.E., Part III*, 1953, 100, 329.
- Harms, F. .. *Ann. d. Phys.*, 1907, 23, 44.
- Kaden, H. .. *Archiv. d. Elek. Ubertragung*, 1951, 5, 534.
- Goubau, G. .. *Proc. I.R.E.*, 1951, 39, 619.
- Dyot, R. B. .. *Proc. I.E.E., Part III*, 1952, 99, 408.
- Buchözl, H. .. *Ann. d. Phys.*, 1940, 37, 173.
- Schorr, M. G. and Beck, F. J. .. *Jour. Appl. Phys.*, 1950, 21, 795.
- King, A. P. .. *Proc. I.R.E.*, 1950, 38, 249.
- Cutler, C. C., King, A. P. and Kock, W. E. .. *Ibid.*, 1947, 35, 1462.
- Chatterjee, S. K., Rama Bai, C. and Shenoy, P. R. .. *Jour. Ind. Inst. Sci.*, 1954, 36, 172.
- Goubau, G. .. *Electronics*, 1954, April, 180.
- Montgomery, C. G. .. *Technique of Microwave Measurements*, 1947, Published by McGraw Hill Co.
- Chatterjee, S. K., Shenoy, P. R. and Rama Bai, C. .. *Jour. Ind. Inst. Sci.*, 1954, 36, 107.
- Burlow, H. M. and Karbowiak, A. E. .. *Proc. I.E.E., Part III*, 1953, 100, 321.
- Burlow, H. M. .. *Ibid., Part III*, 1952, 99, 21.